

1 **Title: Circulating immunome fingerprint in eosinophilic esophagitis is associated**
2 **with clinical response to proton pump inhibitor treatment**

3

4 **Authors:**

5 Lola Ugalde-Triviño^{1,2*}, Francisca Molina-Jiménez^{1,2*}, Juan H-Vázquez^{3*}, Carlos
6 Relaño-Rupérez^{1,2,4}, Laura Arias-González^{2,6,7,8}, Sergio Casabona^{2,9}, María Teresa
7 Pérez-Fernández^{2,9}, Verónica Martín-Domínguez^{2,9}, Jennifer Fernández-Pacheco^{2,9},
8 Alfredo J Lucendo^{2,6,7,8}, David Bernardo^{3,5,&#}, Cecilio Santander^{2,8,9,&#}, Pedro
9 Majano^{1,2,8,10,&#}

10

11 1. Molecular Biology Unit, Hospital Universitario de la Princesa, Madrid, Spain.

12 2. Instituto de Investigación Sanitaria Hospital Universitario de La Princesa (IIS-
13 Princesa), Madrid, Spain.

14 3. Mucosal Immunology Lab, Centro de Investigaciones Biomédicas en Red de
15 Enfermedades Infecciosas (CIBERINFEC), Unidad de Excelencia Instituto de Biología
16 y Genética Molecular (IBGM), Universidad de Valladolid, 47005 Valladolid, Spain.

17 4. Bioinformatics Unit, Centro Nacional de Investigaciones Cardiovasculares (CNIC),
18 Madrid, Spain

19 5. Centro de Investigación Biomédica en Red de Enfermedades Infecciosas
20 (CIBERINFEC), 28029 Madrid, Spain

21 6. Department of Gastroenterology, Hospital General de Tomelloso, Tomelloso, Ciudad
22 Real, Spain.

23 7. Instituto de Investigación Sanitaria de Castilla-La Mancha (IDISCAM), Spain.

24 8. Centro de Investigación Biomédica en Red de Enfermedades Hepáticas y Digestivas
25 (CIBERehd), Madrid, Spain.

26 9. Department of Gastroenterology, Hospital Universitario de La Princesa, Madrid,
27 Spain.

28 10. Department of Cellular Biology, Faculty of Biology, Universidad Complutense de
29 Madrid, Madrid, Spain.

30

31 * Co-first author

32 & Senior author

33 #Correspondence to:

34

35 Pedro L Majano, PhD

36 Hospital Universitario de la Princesa

37 Instituto Investigación Sanitaria Princesa (IP)

38 Diego de León 62

39 28006. MADRID. Spain

40 (pmajano@ucm.es / pedro.majano@salud.madrid.org)

41

42 Dr. Cecilio Santander, MD, PhD

43 Head of Department of Gastroenterology

44 Hospital Universitario de La Princesa

45 Instituto de Investigación Sanitaria Princesa IIS-IP

46 Madrid. Spain

47 (cecilio.santander@salud.madrid.org)

48
49 David Bernardo, PhD
50 Mucosal Immunology Lab, Universidad de Valladolid
51 Unidad de Excelencia Instituto de Biología y Genética Molecular (IBGM)
52 Centro de Investigaciones Biomédicas en Red de Enfermedades Infecciosas
53 (CIBERINFEC)
54 (d.bernardo.ordiz@gmail.com / david.bernardo@uva.es)
55
56

57 **AUTHOR CONTRIBUTIONS**

58 Conceived and designed the study: AJL, DB, CS, PM.
59 Participated in the clinical management of patients: SC, MTF-P, VM-D, JF-P, CS.
60 Performed the experiments: LU-T, FM-J, JH-V, LA-G, PM.
61 Analysed and discussed the data: LU-T, FM-J, JH-V, CR-R, DB, PM.
62 Wrote the paper: LU-T, DB, JH-V, CS, PM.
63 All the authors read, provided comments, and approved the final version of the
64 manuscript.
65

66 **AUTHOR DISCLOSURE**

67 None to declare
68

69 **ORCID NUMBERS**

70 Lola Ugalde-Triviño: 0000-0002-0911-8043
71 Francisca Molina-Jiménez: 0000-0003-4912-1025
72 Juan H-Vázquez: 0000-0002-4805-2403
73 Carlos Relaño-Rupérez: 0000-0002-1407-9245
74 Laura Arias-González: 0000-0003-2132-9350
75 Sergio Casabona: 0000-0002-6131-8341
76 María Teresa Pérez-Fernández: 0000-0003-0363-2516
77 Verónica Martín-Domínguez: 0000-0001-6839-2707
78 Jennifer Fernández-Pacheco 0000-0002-5384-0658
79 Alfredo J Lucendo: 0000-0003-1183-1072
80 David Bernardo: 0000-0002-2843-6696
81 Cecilio Santander: 0000-0001-5492-2535
82 Pedro Majano: 0000-0002-5495-1413
83

84

85

86

87

88

89

90

91 **WHAT IS KNOWN**

- 92
- Eosinophilic esophagitis (EoE) is a Th2 type immune disorder with increased prevalence in the last years.
- 93
- Proton pump inhibitor (PPI) treatment is the preferred first-line therapy for EoE, which leads to clinical and pathological reversion in about half of the cases. Non-responding patients require other therapeutic options.
- 94
- Currently, an endoscopy with esophageal biopsies is required for EoE diagnosis and to monitor response to treatment. Therefore, the discovery of non-invasive biomarkers is of utmost importance for treatment monitoring.
- 95
- To date only peripheral eosinophil and Th2 profiles have been studied in EoE.
- 96
- 97
- 98
- 99
- 100
- 101

102 **WHAT IS NEW HERE**

- 103
- At diagnosis EoE patients have a specific circulating immune signature.
- 104
- PPI-responding and non-responding EoE patients have different immune fingerprints at baseline.
- 105
- Immune characterization of EoE patients at diagnosis and after PPI treatment unveiled differential levels of circulating plasmacytoid dendritic cells (pDCs) depending on their inflammatory state and response to PPI treatment. Those levels are related with the number of pDCs infiltrated in the esophageal tissue.
- 106
- 107
- 108
- 109
- 110

111

112

113

114

115

116

117

118

119

120

121

122

123

124

125

126

127 **ABSTRACT**

128 **Objectives:** The aim of the study was to characterize the circulating immunome of
129 patients with EoE before and after proton pump inhibitor (PPI) treatment in order to
130 identify potential non-invasive biomarkers of treatment response.

131 **Methods:** PBMCs from 19 healthy controls and 24 EoE patients were studied using a
132 39-plex spectral cytometry panel. The plasmacytoid dendritic cell (pDC) population was
133 differentially characterized by spectral cytometry analysis of immunofluorescence
134 assays in esophageal biopsies from 7 healthy controls and 13 EoE patients.

135 **Results:** Interestingly, EoE patients at baseline had lower levels of circulating pDC
136 compared with controls. Before treatment, patients with EoE who responded to PPI
137 therapy had higher levels of circulating pDC and classical monocytes, compared with
138 non-responders. Moreover, following PPI therapy pDC levels were increased in all EoE
139 patients, while normal levels were only restored in PPI-responding patients. Finally,
140 circulating pDC levels inversely correlated with peak eosinophil count and pDC count in
141 esophageal biopsies. The number of tissue pDCs significantly increased during active
142 EoE, being even higher in non-responder patients when compared to responder
143 patients pre-PPI. pDC levels decreased after PPI intake, being further restored almost
144 to control levels in responder patients post-PPI.

145 **Conclusions:** We hereby describe a unique immune fingerprint of EoE patients at
146 diagnosis. Moreover, circulating pDC may be also used as a novel non-invasive
147 biomarker to predict subsequent response to PPI treatment.

148

149 **KEY WORDS**

150 Spectral cytometry, Biomarker, Eosinophilic esophagitis, Plasmacytoid dendritic cells

151

152 **ABBREVIATIONS**

153

154 EoE: Eosinophilic esophagitis

155 EoEHSS: Eosinophilic Esophagitis Histologic Scoring System

156 EREFS: EoE endoscopic reference score

157 GERD: Gastro-esophageal reflux disease.

158 LN: Lymph node

159 LogFC: Log2 Fold Change

160 NR: Non-responder

161 PBMCs: Peripheral blood mononuclear cells

162 pDC: Plasmacytoid dendritic cells

163 PPI: Proton Pump Inhibitors

164 R: Responder

165 Th2: T helper 2 cells

166 UMAP: Uniform Manifold Approximation and Projection

167

168

169

170

171

172 **FINANCIAL SUPPORT**

173 PM and CS are supported by grants PI17/0008 and ISCIII-Proteored 2019 of Instituto
174 de Salud Carlos III (ISCIII, Spain) and co-funded by Fondo Europeo de Desarrollo
175 Regional (FEDER). CS is also funded by Asociación Española de Gastroenterología
176 (AEG) 2019 grant. DB is funded through the Spanish Ministry of Science [PID2019-
177 104218RB-I00], Programa Estratégico Instituto de Biología y Genética Molecular
178 (IBGM Junta de Castilla y León. Ref. CCVC8485) and the European Commission –
179 NextGenerationEU (Regulation EU 2020/2094), through CSIC's Global Health
180 Platform. LU-T is recipient of an INVESTIGO contract from Comunidad de Madrid (09-
181 PIN1-00015.6/2022) partly funded by the European Social Fund, NextGenerationEU,
182 and Recovery, Transformation and Resilience Plan. CR-R is recipient of an
183 INVESTIGO contract from Ministry of Labour and Social Economy, the national public
184 employment service (SEPE) (INVESTIGO Exp. 2022-C23.I01.P03. S0020-0000031)
185 partly funded by the European Social Fund, NextGenerationEU, and Recovery,
186 Transformation and Resilience Plan.

187

188 **ACKNOWLEDGMENTS**

189 We acknowledge, Instituto de Salud Carlos III, FEDER organization, Spanish
190 Gastroenterology Association and Spanish Ministry of Science for the support to this
191 study. Also, we would like to acknowledge the support from European Social Fund,
192 NextGenerationEU, and Recovery, Transformation and Resilience Plan. We express
193 our gratitude to Dr. Manuel Gómez for critical review of the manuscript and English
194 editing.

195

196

197

198 **Word count: 3856**

199

200

201

202

203

204

205

206

207

208

209

210

211

212

213

214

215

216

217

218

219

220

221

222 INTRODUCTION

223

224 Eosinophilic esophagitis (EoE) is a Th2-type immune disorder which is considered an
225 increasing leading cause of chronic esophageal dysfunction in patients of all ages^{1,2}
226 just after gastro-esophageal reflux disease (GERD).

227 Eosinophils are normally found in the gastrointestinal tract; however, they are absent
228 from the esophageal tissue in health conditions. In EoE, the eosinophil infiltrate in the
229 esophageal tissue layers^{3,4} leads to tissue remodelling and fibrosis as well as
230 subsequent dysfunction characterized by esophageal dysmotility, narrowing and
231 rigidity⁵. As a result, patients experience food impaction, dysphagia and heartburn
232 among other symptoms, which impair their health-related quality of life. Therefore, an
233 early EoE diagnosis and effective therapy are essential to prevent impairment of
234 esophageal function. EoE patients often have concurrent allergic responses to food
235 and airborne allergens, together with a yet unexplained male predominance^{6,7}.

236 First-line therapeutic options for EoE include dietary restrictions, protein pump inhibitor
237 (PPI) therapy and swallowed topical corticosteroids, which provide variable
238 effectiveness⁸⁻¹². Recently, the anti-interleukin-4 receptor antagonist dupilumab joined
239 the therapeutic armamentarium against EoE^{13,14}. Among them, PPI represent the
240 preferred therapy in clinical practice, despite its limited effectiveness¹⁵; histologic
241 remission and clinical improvement after PPI are achieved by only 50% and 70% of
242 treated patients, respectively¹⁶. Patients who do not respond to PPI require
243 subsequent therapeutic options.

244 Currently, EoE diagnosis and treatment response monitoring require endoscopy with
245 esophageal biopsies, as clinical symptoms do not correlate well with esophageal
246 inflammation^{17,18}. In this regard, the chronic nature of this disease together with the
247 dissociation between patients' symptoms and esophageal inflammation¹⁸ require
248 seeking for novel reliable biomarkers and clinical parameters able to identify patient
249 profiles at diagnosis and follow-up. Recent studies have focused on seeking for new
250 biomarkers by characterizing the RNA¹⁹⁻²¹ and proteomic profile of EoE at esophageal
251 tissue level²². Nevertheless, these approaches are still invasive. Hence, the
252 development of novel non-invasive biomarkers to aid on EoE diagnosis and monitoring
253 is an essential unmet need²³.

254 Building from all these precedents, in this study we aimed to characterize the
255 circulating immunome of EoE patients at the time of diagnosis using top-of-the-art
256 spectral cytometry. With this approach, we expected to identify specific immune
257 subsets that could not only help to characterize this disorder, but also to identify novel
258 non-invasive biomarkers able to predict response to PPI treatment.

259

260

261 MATERIAL AND METHODS

262

263 Human subjects

264

265 A total of 25 incident adult EoE patients were prospectively recruited at the moment of
266 diagnosis at Hospital Universitario de La Princesa (Madrid, Spain) between February
267 2018 and November 2020. EoE was diagnosed according to evidence-based

268 guidelines³ including: (i) symptoms referring to esophageal dysfunction, (ii) infiltration of
269 the esophageal epithelium by 15 or more eosinophils per high-powered field (hpf)
270 assessed from 6 endoscopic biopsy samples; (ii) absence of eosinophilic infiltration in
271 biopsy specimens from gastric and duodenal mucosa; and (iii) exclusion of alternative
272 potential causes of esophageal eosinophilia. Subjects (n=19) who underwent upper
273 endoscopy for assessment of dyspepsia or suspected gastroduodenal ulcer were
274 included as controls. Esophageal biopsies obtained in the endoscopy were normal in
275 all cases and eosinophilic infiltration was excluded. All controls with hiatus hernia,
276 incompetent cardias, or esophageal peptic lesions were excluded hence ensuring that
277 all the recruited controls displayed a normal endoscopic appearance and eosinophil-
278 free biopsies of the esophagus.

279 Atopic background was recorded for all EoE patients and control subjects. The EoE
280 endoscopic reference score (EREFS) rating the severity of esophageal inflammation
281 (oedema, furrows, exudates) and fibrosis (rings and stricture)²⁴ was assessed in all
282 patients. Furthermore, the validated Eosinophilic Esophagitis Histologic Scoring
283 System (EoEHSS) was also determined, evaluating eight pathologic features for both
284 severity (grade) and extent (stage) of abnormalities²⁵.

285 Out of the 25 EoE patients, 18 underwent double dose PPI treatment (omeprazole 20
286 mg b.i.d. or equivalent) for an 8-week period, after which they were classified as
287 responders (n=9) or non-responders (n=9) based on the peak eosinophil count in a
288 second endoscopy in which EREF and EoEHSS scores were also assessed. The study
289 was approved by the local Ethics Committee (PI17/0008, registry number 3107, 8 June
290 2017). All individuals provided written informed consent.

291

292 **Blood samples**

293 In all cases, blood samples were obtained at the time of the endoscopy from EoE
294 patients (both before and after PPI-treatment in the latter) and controls. After placing a
295 venous line to provide sedation for endoscopy, blood was collected in EDTA-coated
296 tubes to isolate peripheral blood mononuclear cells (PBMC).

297

298 **PBMCs staining and spectral cytometry acquisition**

299 PBMCs were isolated by Ficoll gradient assay. Viable cells were counted and
300 cryopreserved in freezing medium (Foetal bovine serum [Hyclone,Thermofisher]
301 complemented with DMSO 20% medium) at vapour phase of liquid nitrogen.

302 For the analysis, PBMCs were thawed and a total of 2 million PBMCs were stained with
303 monoclonal antibodies (Supplementary Table 1) applying a modified OMIP-69 panel
304 protocol²⁶. Before staining, Live/Dead fixable blue dead cell stain kit was added to
305 exclude dead cells from the analysis. Brilliant Stain Buffer and True-Stain Monocyte
306 Blocker were also added before staining with the aim of obtaining the optimal
307 fluorescence. PBMCs were washed with FACS buffer (500mL PBS +1 0mL filtered
308 FCS + 0.1g NaN₃ + 2.5mL sterile EDTA) and incubated in the dark at room
309 temperature during staining. Cells were further fixed in 0.8% paraformaldehyde in
310 FACS buffer in the dark for 10min and washed with FACs buffer. Cells were preserved
311 at 4°C until acquired (within 48h) in a 5-laser spectral cytometer (Aurora, Cytek).

312

313 **Cytometry data and statistical analysis**

314 Spectral cytometry data were analysed using the OMIQ Data Science platform (©
315 Omiq, Inc. 2022). After setting the scale, parameters, and cofactors, the FlowAI

316 algorithm was used for cleaning the data from aberrant signal patterns or events. Then,
317 cell debris and doublets were excluded to gate viable leukocytes (CD45⁺) where an
318 unsupervised approach was applied with a dimensionality reduction Uniform Manifold
319 Approximation and Projection (UMAP)²⁷ plus clustering FlowSOM algorithms. Merging
320 these two algorithms allows a deeper classification of the different immune subsets
321 through different marker expression on the UMAP. A heatmap was also built showing
322 the expression levels of each marker within each cluster. Dendrograms further grouped
323 the clusters and markers associated by similarity.
324 Statistical analysis was performed in all cases using Rstudio 2022.07.2+576.
325 Differential analysis of clusters defined in OMIQ was performed with the edgeR
326 package, using genewise quasi-likelihood (QL) F-tests with GLMs. Significance was set
327 at p-value ≤ 0.05 and Log2 Fold Change (LogFC) ≥ 1.5. Differences between groups of
328 significant clusters were validated by classic gating strategy approaches
329 (Supplementary Figure 1 and 2). Manual gating results were analysed by *t*-test (paired
330 when indicated) and/or two-way ANOVA test followed by *post hoc* Fisher test. Outliers
331 were determined through Grubbs' test and deleted from the final analysis. Statistical
332 significance was considered when p-value ≤ 0.05 in all cases (p < 0.05 *, p < 0.01 **,
333 p < 0.001 ***, p < 0.0001 ****, n.s. = not significant). Percent of total always refers to
334 percentage of cells of the specified population relative to total PBMCs.

335

336 **Immunofluorescence staining in esophageal biopsies**

337

338 Immunofluorescence staining was performed in biopsies from control subjects and EoE
339 patients, previously oriented in a cellulose acetate and included in paraffin-embedded
340 blocks, using the antibodies CD123-biotin (Stem Cell, 60110BT), HLA-DR (Santa Cruz,
341 sc-53319) and CD11c (Thermo Fisher Scientific, PA535326). Briefly, slides with 4-µm
342 sections of esophageal biopsies, underwent deparaffinization, antigen retrieval using
343 sodium citrate buffer (pH 6.0), blocked with 4% goat serum/phosphate-buffered saline
344 (PBS), and then incubated with primary antibody (HLA-DR and CD11c) diluted in 1%
345 goat serum-PBS overnight at 4 °C in a humidified chamber. Then, slides were washed
346 with PBS + 1% NP-40 and incubated with secondary antibodies diluted in 1% goat
347 serum-PBS for 30min at RT in a humidified chamber. After, slides were washed with
348 PBS + 1% NP-40 and incubated with primary antibody (CD123) diluted in 1% goat
349 serum/PBS overnight at 4 °C in a humidified chamber. Finally, slides were washed in
350 PBS + 1% NP-40 and incubated with secondary antibodies and DAPI (0.5 µg/mL)
351 diluted in 1% goat serum/PBS for 30min at RT in a humidified chamber. Finally, a cover
352 slip was added with ProLong Gold mounting reagent (Molecular Probes). Images were
353 obtained using a Thunder Imager (Leica) with LAS X software and analysis was done
354 using ImageJ and RStudio software. Normality was assessed by Saphiro Wilk
355 normality test, the non-parametric Mann-Whitney test was done to compare between
356 pairs of groups. In all cases (p < 0.05 *, p < 0.01 **, p < 0.001 ***, p < 0.0001 ****, n.s. = not
357 significant).

358

359 **RESULTS**

360

361 **Patient Demographics**

362 Clinical and demographic characteristics of study participants are summarized in Table
363 1. Compared to controls (n=19), EoE patients (n=25) were older (34 vs 41 years) and
364 more frequently male (68% vs 88%), but no significant differences were found in
365 demographic characteristics across groups.

366 EoE patients treated with PPI (n=18) were classified as responders or non-responders
367 to the therapy. EoE remission was defined as presenting a peak eosinophil count
368 below 15 after at least 8 weeks of treatment. Response to PPI was also associated
369 with improvement in EoE symptoms from baseline (assessed as patient reported
370 outcomes), as well as in endoscopic and histologic characteristics, assessed with the
371 scores EREFS and Grade and Stage EoEHSS, respectively. Baseline characteristics of
372 PPI responding, and non-responding patients showed no differences.

	Control (n=19)	EoE (n=25)	p-value	Responders (n=9)	Non-Responders (n=9)	p-value
Sex (male) (n,%)	13 (68%)	20 (80%)	0.488	7 (77%)	7 (77%)	1
Age (mean years ± s.d.)	34.42 ± 10.93	41 ± 13.7	0.060	33 ± 12.85	44 ± 14.95	0.152
<i>Symptoms (n,%)</i>						
Dysphagia	0	23 (92%)	<0.001	9 (100%)	9 (100%)	1
Food impaction	0	16 (64%)	<0.001	7 (77%)	5 (55%)	0.819
Heartburn	0	10 (40%)	0.002	3 (33%)	3 (33%)	1
Abdominal pain	0	0 (0%)	1	0 (0%)	0 (0%)	1
<i>Any atopic disease (n,%)</i>						
Atopic diseases	1 (5%)	20 (87%)	<0.001	8 (88%)	9 (100%)	1
Asthma	0	5 (22%)	0.053	3 (33%)	1 (11%)	0.573
Allergic rhinitis/sinusitis	1 (5%)	19 (82%)	<0.001	8 (88%)	9 (100%)	1
Food allergy	2 (10%)	11 (48%)	0.0173	5 (55%)	3 (33%)	0.637
<i>Endoscopic findings (n,%)</i>						
EREFs (mean ± s.d.)	0	3.36 ± 2	<0.001	2.44 ± 2.06	3.88 ± 1.26	0.097
EREFs PostPPI (mean ± s.d.)	-	-	-	1.44 ± 1.51	4.33 ± 1	<0.001
Maximum eosinophil count (mean ± s.d.)	0	55.66 ± 23.9	<0.001	46.22 ± 21.76	65.56 ± 19.43	0.064
Maximum eosinophil count PostPPI (mean ± s.d.)	-	-	-	1.44 ± 2	65 ± 20.91	<0.001
<i>Histological findings</i>						
EoEHSS Grade (0-1) (mean ± s.d.)	0	0.50 ± 0.19	<0.001	0.43 ± 0.22	0.57 ± 0.15	0.122
EoEHSS Grade (0-1) PostPPI (mean ± s.d.)	-	-	-	0.06 ± 0.04	0.40 ± 0.22	0.006
EoEHSS Stage (0-1) (mean ± s.d.)	0	0.47 ± 0.16	<0.001	0.43 ± 0.17	0.57 ± 0.15	0.122
EoEHSS Stage (0-1) PostPPI (mean ± s.d.)	-	-	-	0.02 ± 0.03	0.31 ± 0.19	0.007
<i>PPI Treatment</i>						
Omeoprazol	-	-	-	6 (66%)	2 (22%)	0.1385
Esomeprazol	-	-	-	2 (22%)	2 (22%)	
Pantoprazol	-	-	-	1 (11%)	5 (55%)	

373

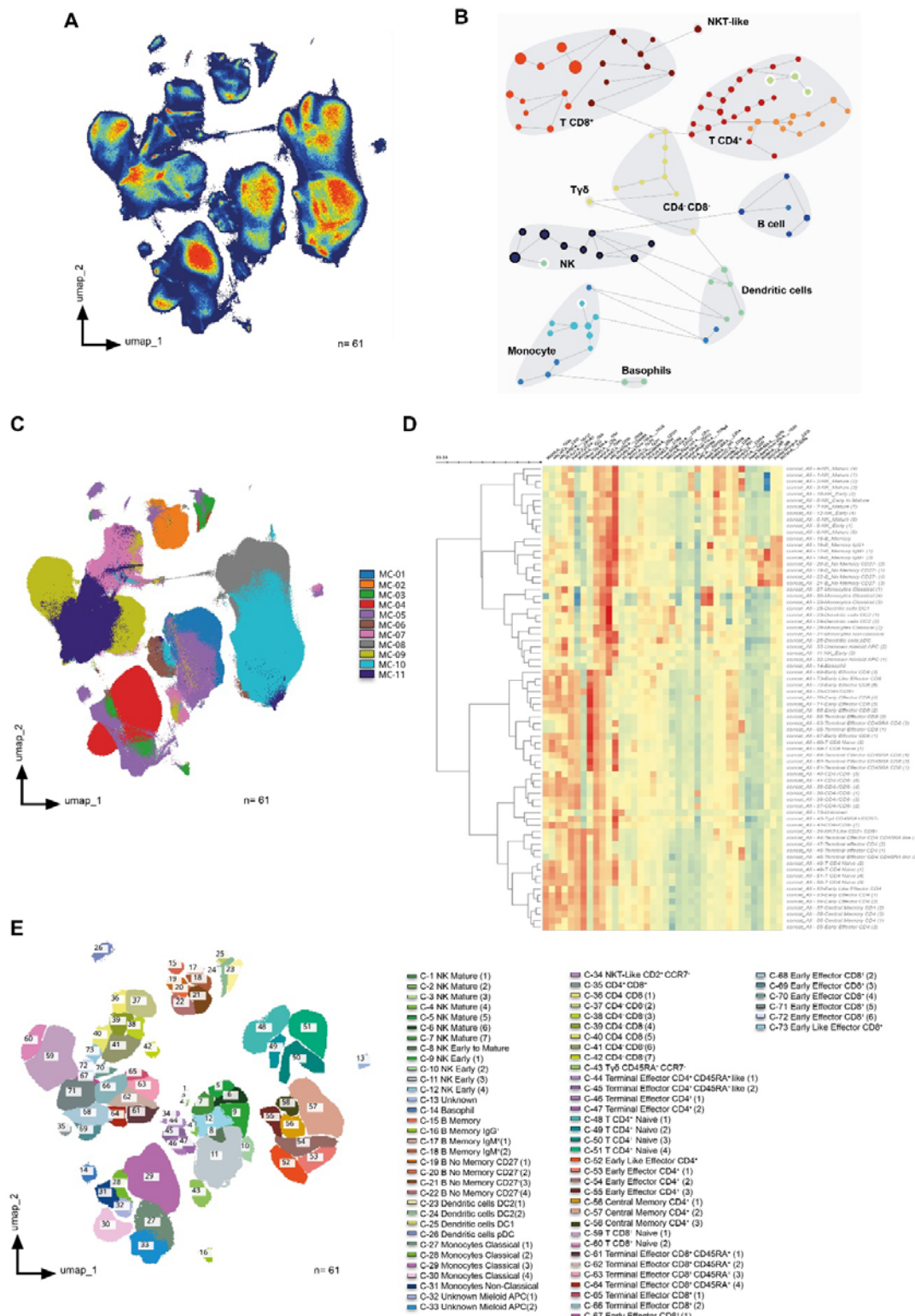
374 **Table 1. Clinical features of controls and EoE patients.** Fisher's test and *t*-test were
375 applied to analyse differences between control and EoE patients and between
376 responders and non-responders. P-value is shown for each comparison. Abbreviations:
377 EoE: Eosinophilic Esophagitis; EoEHSS: Eosinophilic Esophagitis Histologic Scoring
378 System; EREFS: EoE endoscopic reference score; PPI: Proton Pump Inhibitors.

379 **High dimensional analysis on PBMCs from controls and EoE patients**

380 A total of 61 samples (19 controls, 24 patients at disease onset, as well as 9
381 responders and 9 non-responders to PPI after 8-week treatment) were analysed by
382 UMAP identifying four major continents and several smaller islands (Figure 1A). The
383 relative expression of each marker on the UMAP (Supplementary Figure 3) revealed
384 that the main continent on the left represents cytotoxic (CD8⁺) T-cells together with
385 double negative (CD4⁻CD8⁻) T-cells. On the other hand, the main continent on the right
386 is composed of helper (CD4⁺) T-cells. Likewise, the island on the bottom is mainly
387 composed of monocytes, basophils and myeloid antigen presenting cells (APC), while
388 the islands in the middle represent NK cells and $\gamma\delta$ T-cells. B-cells are represented in
389 the top island together with dendritic cells.

390

391 To further refine the analysis, FlowSOM algorithm was applied to find similar cell
392 subsets and separate them into metaclusters in an unsupervised manner (Figure 1B).
393 The overlay of the FlowsSOM clustering on the UMAP representation (Figure 1C)
394 allowed us to perform a more exhaustive analysis, identifying a total of 73 clusters
395 according to surface marker expression as shown in the heatmap (Figure 1D).
396 Supplementary Table 2 shows an in-depth characterization of the phenotype of all
397 clusters, which allowed the identification of 70 of them, since clusters 13, 32 and 33
398 could not be clearly identified. Finally, all clusters were further uploaded into the UMAP
399 (Figure 1E) to determine not only how they relate to each other, but also to display their
400 pseudoevolution.



401
402
403
404
405
406

Figure 1. High dimensional analysis of peripheral blood mononuclear cells from controls and EoE patients.

(A) UMAP density analysis representation performed on singlets corresponding to total viable circulating CD45⁺ cells from all samples. Samples were obtained from 19 controls and 24 patients at disease onset, as well as 9 responders and 9 non-

407 responders to PPI therapy after 8-week treatment (a total of 61 samples). **(B)**
 408 FlowSOM clustering on total viable singlet CD45⁺ cells identified the main metaclusters
 409 on dataset: B-cells, NK cells, $\gamma\delta$ T-cells, CD4⁺ T-cells, CD8⁺ T-cells, dendritic cells,
 410 basophils, monocytes, CD4⁻CD8⁻ T-cells, and NKT-like cells. **(C)** UMAP representation
 411 of all samples after non-supervised FlowSOM clusterization **(D)** Heatmap displaying
 412 the relative expression of each marker within each of the 73 identified clusters.
 413 Euclidean distance between clusters was calculated and represented by the
 414 dendrogram at the left side of the plot. **(E)** All 73 identified clusters were overlaid on the
 415 UMAP projection. Each identified cluster is tagged by a specific colour and number as
 416 shown in the legend.

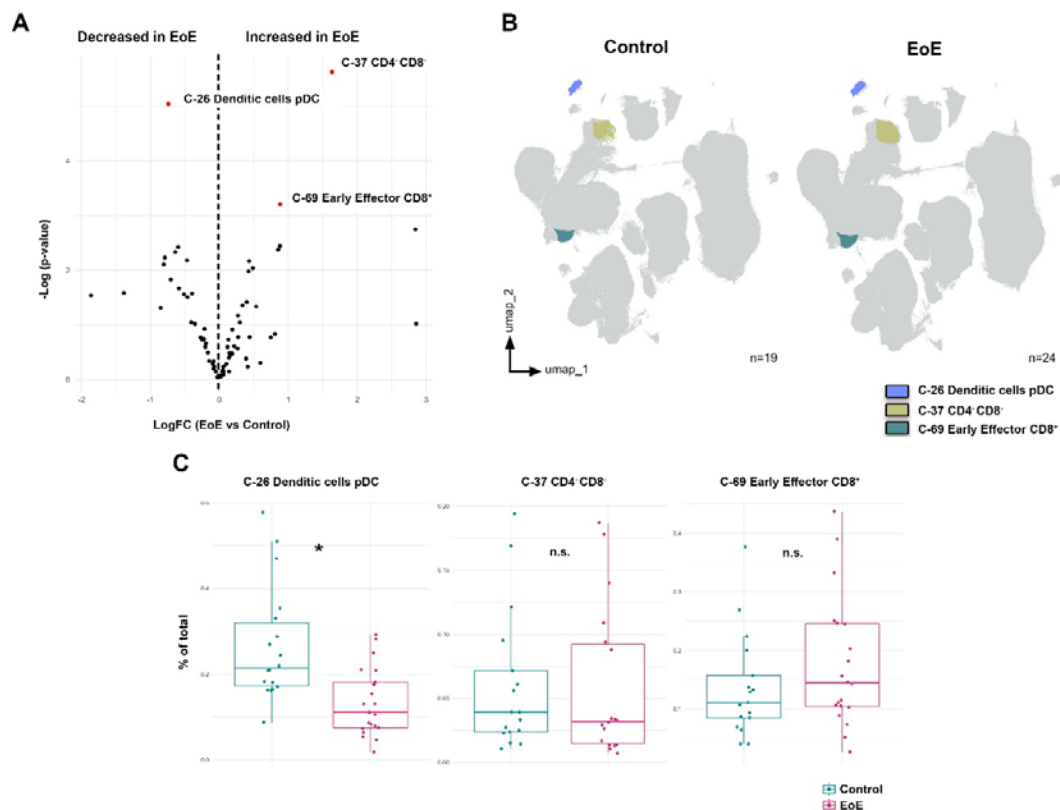
417

418

419 Peripheral immune profile differs between EoE patients and controls at baseline 420 visit

421 After characterizing the different clusters, or immune subsets, present in our samples,
 422 we next addressed the immune differences found between controls and EoE patients
 423 at baseline visit. Volcano plot representation (Figure 2A) showed a significant deficit of
 424 plasmacytoid dendritic cells (pDC) (C-26) in EoE patients and an expansion of CD4⁻
 425 CD8⁻ and early effector CD8⁺ T-cells (Clusters 37 and 69) at the time of disease
 426 diagnosis (Figure 2B). In order to further confirm these findings, classical gating
 427 strategies were applied as shown in Supplementary Figure 2, hence confirming that
 428 EoE patients display a deficit of circulating pDC at disease onset (Figure 2C).

429



430

431 **Figure 2. Peripheral immune profile differs between EoE patients and controls at**
 432 **baseline visit.**

433 **(A)** Volcano plot analysis comparing clusters from controls (n=19) and patients with
434 eosinophilic esophagitis at disease diagnosis (EoE, n=24). LogFC and -Log(p-value)
435 are shown. Clusters considered statistically significant are shown in red together with
436 their nature as elucidated from Supplementary Table 2. **(B)** These differentially
437 expressed clusters between control and EoE patients are further shown in the UMAP
438 representation. **(C)** Validation of these clusters was performed following classical
439 gating approaches (Supplementary Figure 1 and 2). *t*-test was applied in panel D,
440 considering a p-value <0.05 as statistically significant (*p<0.05). Percent of total always
441 refers to percentage of cells of the specified population relative to total PBMCs.

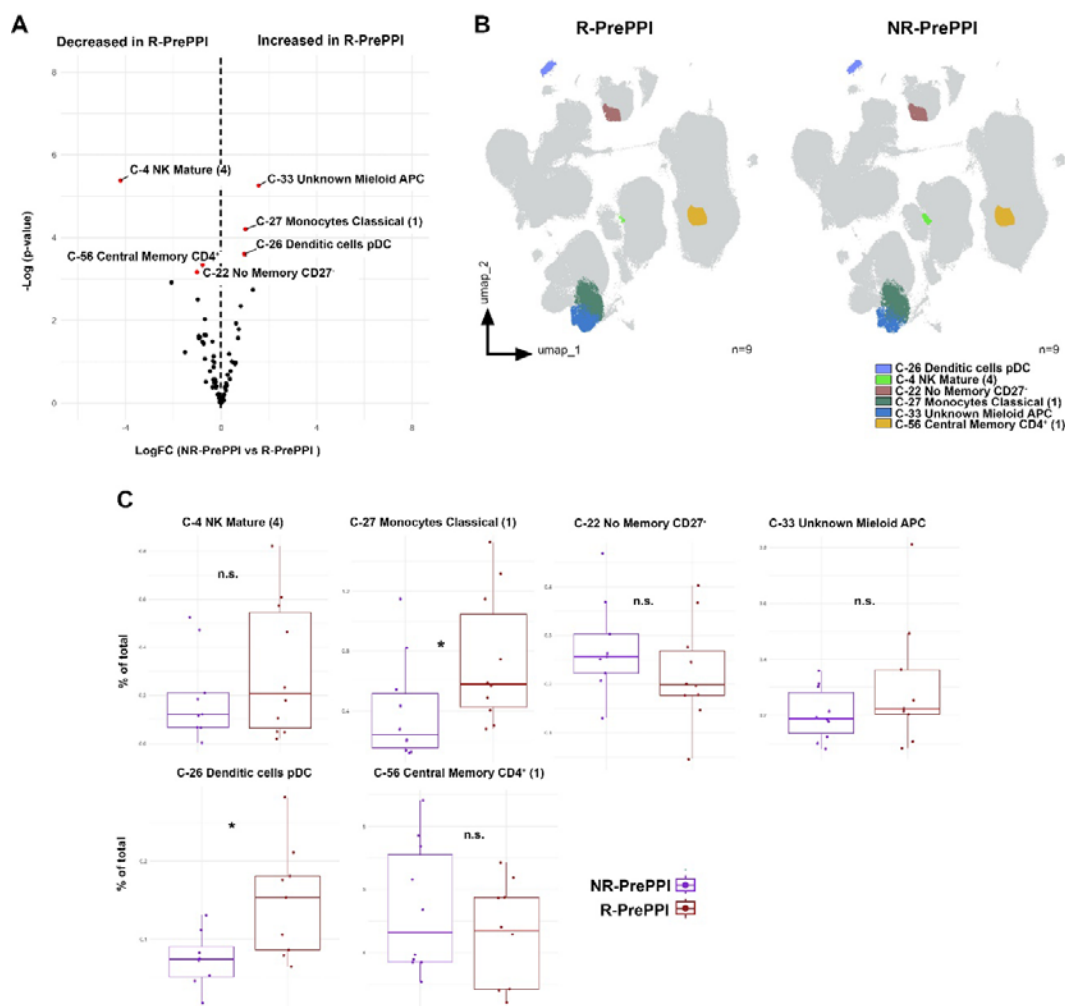
442

443 **Circulating pDC and classical monocyte levels at baseline are associated to PPI**
444 **response.**

445

446 After describing that 3 clusters were differentially expressed on EoE patients at disease
447 diagnosis, with a specific reduction of circulating pDCs as confirmed by classical gating
448 approaches, we next aimed to address whether we could also identify specific clusters
449 that might predict patient's response to PPI treatment.

450 To that end, we compared the immune profile of responding (R) and non-responding
451 (NR) patients (Table1) at disease onset (i.e., before PPI treatment [PrePPI]) (Figure
452 3A). Our results revealed that responding patients at diagnosis had higher levels of
453 circulating pDC, myeloid antigen presenting cells and classical monocytes; together
454 with lower levels of mature NK cells, and no memory B-cells and central memory CD4⁺
455 T-cells (Figures 3B and 3C). Of note, further analysis following classical gating
456 approaches confirmed that PPI-responding patients had higher levels of circulating
457 pDC and classical monocytes at disease onset compared to non-responders (Figure
458 3D).



459

460

Figure 3. Circulating pDC and classical monocyte levels are associated to PPI response at disease diagnosis

461

(A) Volcano plot of differential analysis between responding (R, n=9) and non-responding patients (NR, n=9). LogFC and -Log(p-value) at baseline are shown.

462

Clusters considered statistically significant are highlighted in red, showing their name and number. (B) UMAP representation from R and NR patients, in which significant clusters are coloured.

463

(C) Validation by classic gating (Supplementary Figure 1 and 2) of the significant clusters previously defined. Boxplots of significant clusters represent individual percentage of total value, group medians as well as minimum and maximum values.

464

Differences were analysed by *t*-test considering p-values <0.05 as statistically significant (**p*<0.05, ***p*<0.01, ****p*<0.001, *****p*<0.0001) (R n=8, NR n=7). Responder (R), Non-Responder (NR), before treatment (PrePPI). Percent of total always refers to percentage of cells of the specified population relative to total PBMCs.

465

466

467

468

469

470

471

472

473

Circulating pDC levels are restored in PPI-responding patients following treatment

474

475

476

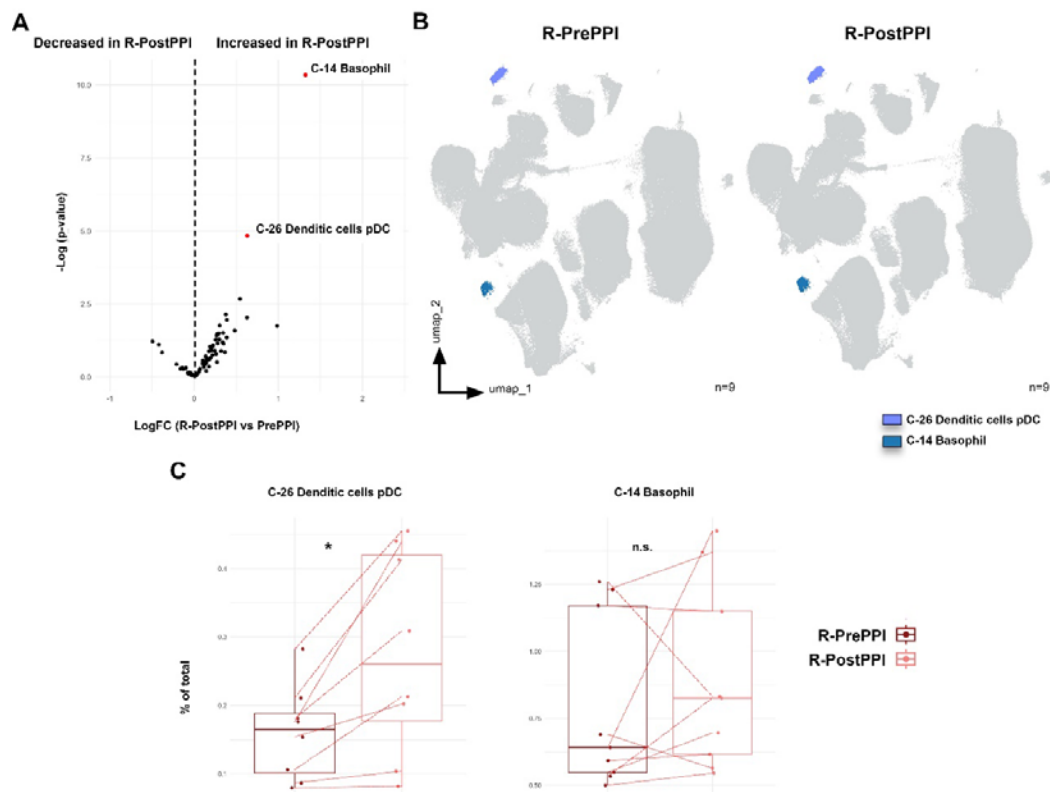
Since patients with PPI responsive and non-responsive EoE displayed different immune cell levels at the time of disease diagnosis, we next aimed to address whether we could also identify specific clusters modulated by PPI treatment. To that end, we

477

478

479

480 next compared the profile of EoE responsive (R) patients both before (PrePPI) and
481 after (PostPPI) PPI therapy (Table1).
482 Our results revealed that, following treatment, circulating levels of pDC (C-26) and
483 basophils (C-14) were increased in PPI-responding patients (Figures 4A and 4B),
484 something particularly relevant in the case of circulating pDC as that increase was
485 further confirmed by classical gating approaches (Figure 4C).
486 Based on these observations, we also assessed the immune cell dynamics in non-
487 responding patients (Supplementary Figure 4A). The pDC cluster was increased in
488 these patients following treatment (Supplementary Figure 4B); however, that
489 observation could not be confirmed following classical gating strategy (Supplementary
490 Figure 4C). Therefore, taken all together our results suggest that clinical response to
491 PPI-treatment is associated with an increase in circulating pDC levels.
492



493

494

495 **Figure 4. pDC and basophil levels are increased in responding patients upon PPI**
496 **treatment.**

497 **(A)** Volcano plot analysis of the clusters comparing patients responding to proton pump
498 inhibitor (PPI) treatment, both before (R-PrePPI) and after (R-PostPPI) therapy. LogFC
499 and -Log(p-value) are shown. Clusters considered statistically significant are shown in
500 red together with their nature as elucidated from Supplementary Table 2. **(B)** UMAP
501 representation of these differentially expressed clusters in R-PrePPI and R-PostPPI.
502 **(C)** Further validation of these clusters was performed following classical gating
503 approaches as shown in Supplementary Figure 1 and 2. Boxplots of significant clusters
504 represent individual percentage of total value, group medians as well as minimum and
505 maximum values. Red line indicates paired PrePPI and PostPPI samples. Differences

506 were analysed by paired *t*-test considering p-values <0.05 as statistically significant
507 (*p<0.05, **p< 0.01, ***p< 0.001, ****p<0.0001) (n=8). Responder (R), before PPI
508 treatment (PrePPI), after PPI treatment (PostPPI). Percent of total always refers to
509 percentage of cells of the specified population relative to total PBMCs.

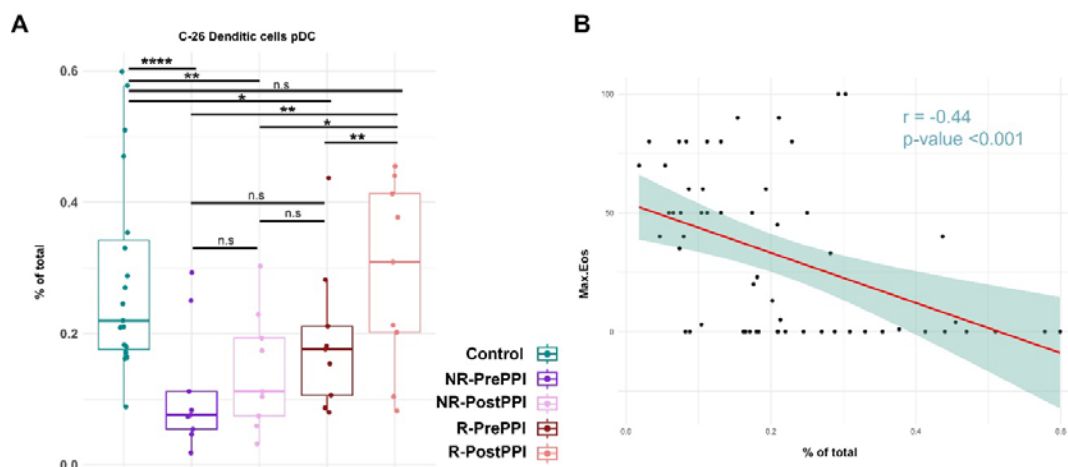
510

511 **Circulating pDCs are associated with EoE pathology and PPI-response**

512 Having described that pDCs are differentially decreased in EoE patients at the moment
513 of diagnosis, (Figure 2) while within EoE patients they are higher in those who respond
514 to PPI treatment (Figure 3) and, indeed, they are further increased following such
515 clinical intervention (Figure 4) although not in non-responding patients (Supplementary
516 Figure 4), we next decided to focus on this cell population. Hence, further analysis
517 confirmed that all EoE patients had lower levels of circulating pDCs at diagnosis,
518 although these levels were lower in non-responding patients than in responders.
519 Furthermore, in responders pDC levels were indeed further restored to control levels
520 following treatment.

521 Since pDCs seem to be related to disease remission, we next hypothesized that cells
522 might be correlated with the esophageal inflammatory state of the patient. To test this
523 hypothesis, we studied the correlation between the maximum eosinophil count in the
524 esophageal biopsy and pDC levels (Figure 5B). We found a negative correlation ($r =$
525 0.44 p-value= <0.001), suggesting the implication of pDCs in EoE pathogenesis.

526



527

528 **Figure 5. Circulating pDC are associated with EoE pathology and PPI-response**

529 **(A)** Boxplots represent levels of pDC in control and EoE patients before and after PPI
530 treatment, as individual percentages of total counts as well as group medians and
531 minimum and maximum values. Differences were analysed by *t*-test, considering p-
532 values <0.05 as statistically significant. **(B)** Pearson correlation between pDC and peak
533 eosinophil count. Pearson correlation coefficient and p-value are shown. (Control n=19,
534 R n=9, NR n=9). Responder (R), Non-Responder (NR), before PPI treatment (PrePPI),
535 after PPI treatment (PostPPI) (*p<0.05, **p< 0.01, ***p< 0.001, ****p<0.0001).

536

537

538

539

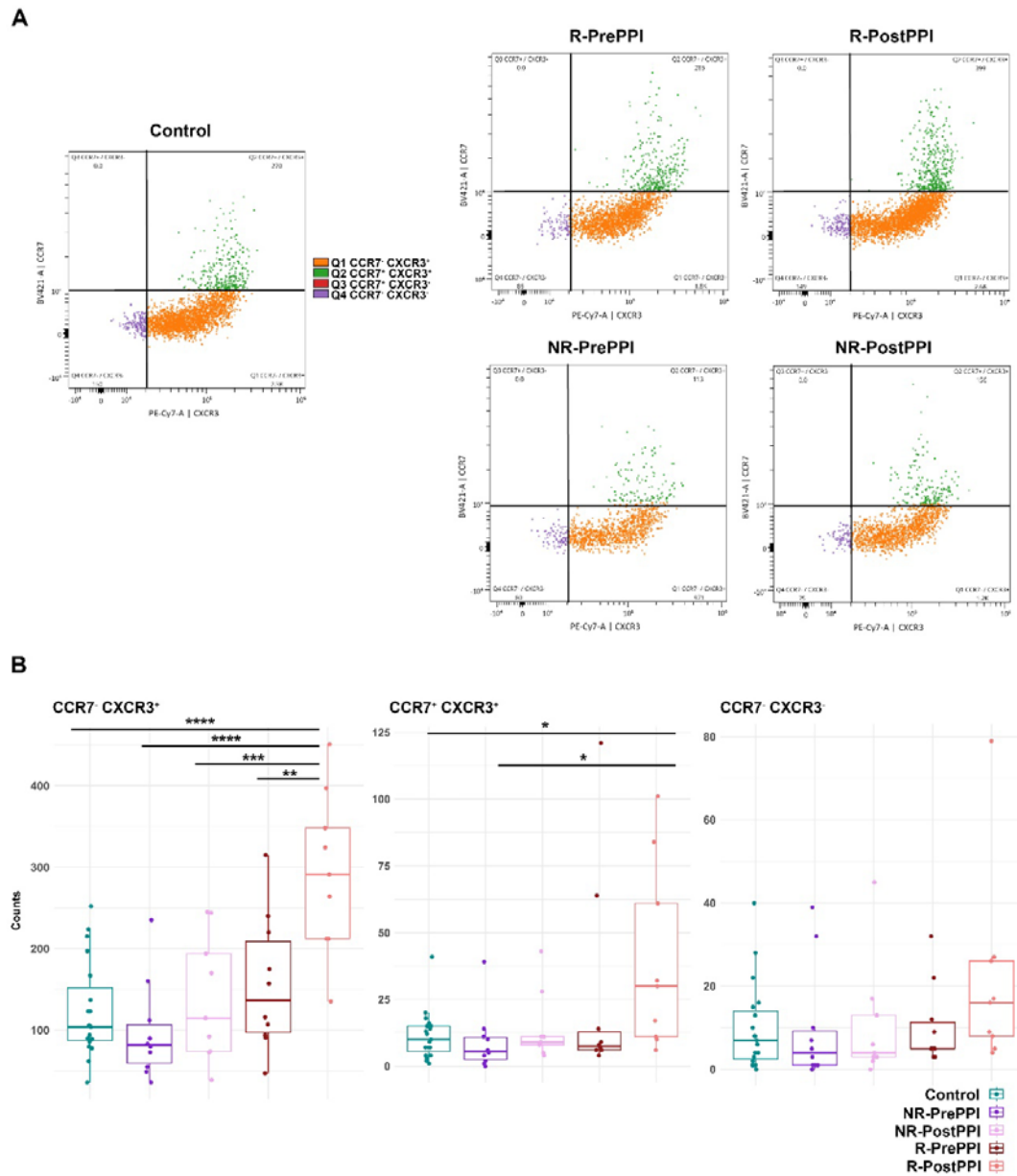
540

541

542
543
544
545
546
547
548
549
550
551

Differential activation profile of circulating pDCs in EoE and remission

Next, we assessed the expression of the chemokine receptors CCR7 and CXCR3 on circulating pDC, as they mediate pDC migration towards the lymph nodes (LN) and peripheral sites of inflammation^{28,29} (Figure 6A). CXCR3⁺ pDC (either CCR7⁺ or CCR7⁻) were increased in PPI responding patients following treatment (Figure 6B) suggesting a potential mechanism of action for pDC related with their infiltration in the esophagus.



552
553
554
555

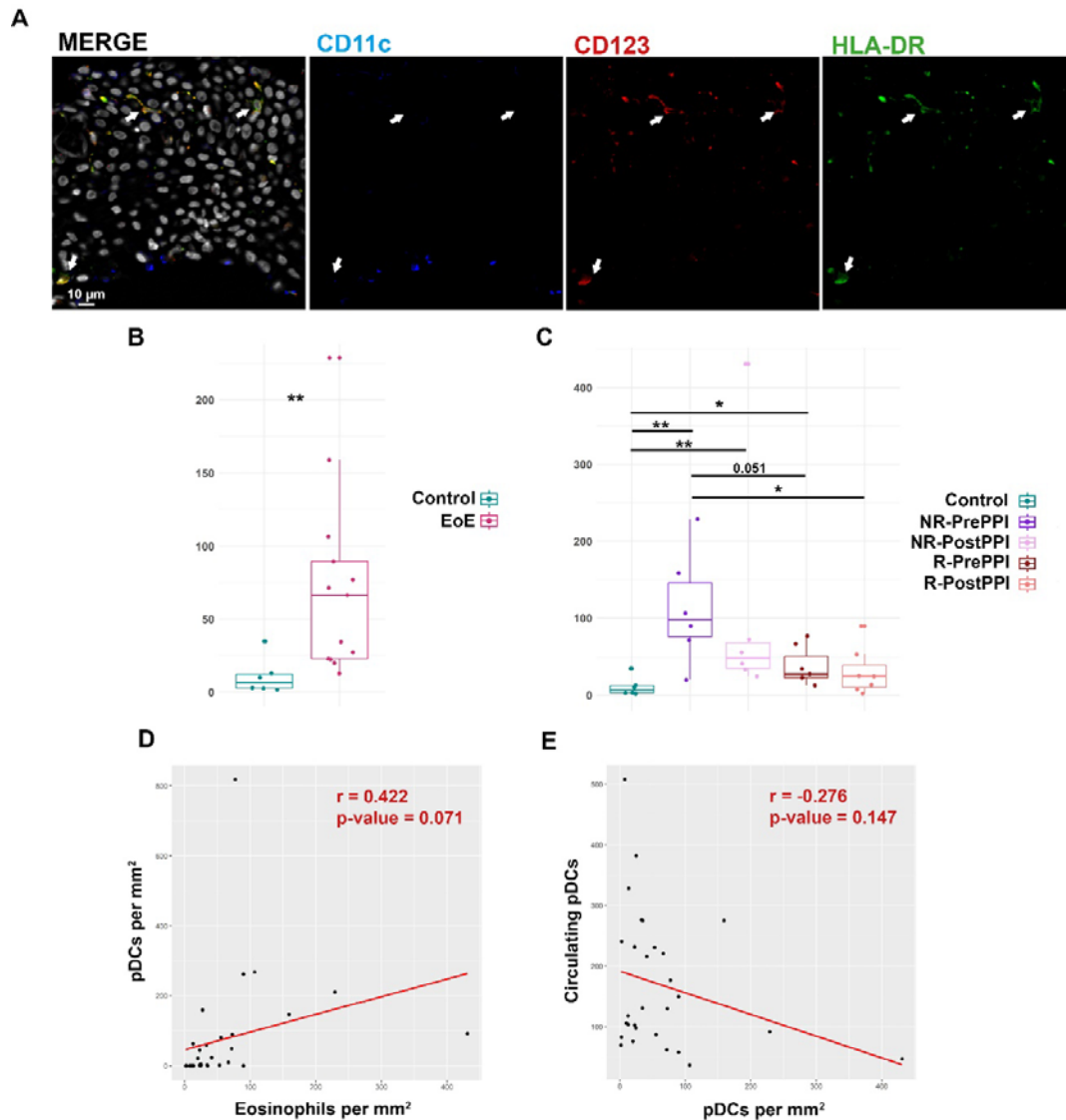
Figure 6. Differential activation profile of circulating pDC in EoE and remission. (A) Gating of activated pDC subpopulations according to their CCR7 and CXCR3

556 expression: CCR7⁻/CXCR3⁺(blue), CCR7⁺/CXCR3⁺ (orange), CCR7⁺/CXCR3⁻ (green),
557 CCR7⁻/CXCR3⁻ (red). Dot plots show representative distribution of these
558 subpopulations in each cohort. **(B)** Boxplot representation of the different pDC
559 activation profiles in the five cohorts . Total count, group median and minimum and
560 maximum values are represented. Differences were analysed by multiple comparison
561 ANOVA followed by *post hoc* Fisher's test, considering p-values <0.05 as statistically
562 significant (*p<0.05, **p< 0.01, ***p< 0.001, ****p<0.0001). (Control n=19, R n=9, NR
563 n=9). Responder (R), Non-Responder (NR), before treatment (PrePPI), after treatment
564 (PostPPI).
565

566 **pDC infiltration in esophageal biopsies of EoE patients**

567
568 Finally, after describing the activation profile of the circulating pDC population, we
569 studied by immunofluorescence assay the infiltration of these cells in esophageal
570 biopsies of 7 healthy controls and 13 EoE patients (6 R and 7 NR) before and after PPI
571 treatment (Figure 7). pDCs were characterized as CD123⁺ (red) HLA-DR⁺ (green)
572 CD11c⁻ (blue) cells and quantified per mm² of tissue (Figure 7A). The number of tissue
573 pDCs was significantly higher in EoE patients than in controls (Figure 7B), being higher
574 in NR-prePPI when compared to R-prePPI (Figure 7C). The number of tissue pDCs
575 was reduced in NR and R patients after PPI treatment although differences were not
576 statistically significant. However, R-postPPI values were the closest to those of
577 controls (Figure 7C).

578 In general, tissue pDCs inversely correlated with the circulating pDC count and were
579 directly related with the number of eosinophils per mm² (Figure 7D,E). Thus, levels of
580 this immune population seem to be related with PPI-response and EoE activity.



581

582 **Figure 7. pDC infiltration in esophageal biopsies of EoE patients (A)**
 583 Immunofluorescence analysis of pDC infiltrate in esophageal biopsies from EoE
 584 patients. pDCs were visualized as CD123⁺(red) CD11c⁻ (blue), HLA-DR⁺ (green) cells.
 585 Arrows point to representative examples of pDC. Scale bar is shown. Nuclei were
 586 stained with DAPI (represented in grey in merged images). **(B)** Boxplot representation
 587 of infiltrating pDCs in controls (n=7) and EoE (n=13) patients at baseline. Relative
 588 count per mm^2 , group median and minimum and maximum values are represented.
 589 Differences were analysed by Mann-Whitney test, considering p-values <0.05 as
 590 statistically significant (*p<0.05, **p< 0.01, ***p< 0.001, ****p<0.0001). **(C)** Boxplot
 591 representation of infiltrating pDCs in controls (n=7), responder (n=6) and non-
 592 responder (n=7) pre-PPI and post-PPI. Relative count per mm^2 , group median and
 593 minimum and maximum values are represented. Differences were analysed by Mann-
 594 Whitney test, considering p-values <0.05 as statistically significant (*p<0.05, **p< 0.01,
 595 ***p< 0.001, ****p<0.0001). Responder (R), Non-Responder (NR), before treatment
 596 (PrePPI), after treatment (PostPPI). **(D)** Pearson correlation between tissue eosinophil
 597 count and tissue pDCs. Pearson correlation coefficient and p-value are shown. **(E)**

598 Pearson correlation between circulating pDC and tissue pDCs. Pearson correlation
599 coefficient and p-value are shown.
600

601 DISCUSSION

602 Using state-of-the-art spectral cytometry, we hereby describe, for the first time to our
603 knowledge, a unique fingerprint in the circulating immunome of patients with EoE at the
604 time of disease diagnosis characterized by a specific deficit of circulating pDCs.
605 Indeed, their levels were further decreased at diagnosis in patients who did not
606 respond to PPI treatment, while among those who did, circulating levels of this cell
607 subset were restored to normal levels upon treatment. Moreover, when we evaluated
608 the presence of pDCs in the esophagus their numbers correlated with the eosinophilic
609 count, showing both an inverse correlation with circulating pDCs. Hence, our findings
610 suggest a central role of pDCs in the pathogenesis of EoE and reveal them as potential
611 novel non-invasive biomarkers to aid on disease diagnosis and predict subsequent
612 response to PPI therapy.

613 In addition to our novel findings on pDCs, we found an increase in CD4⁺CD8⁻ T-cells
614 and CD8⁺ Early Effectors (C-37 and C-69, respectively) in EoE patients at diagnosis,
615 although these results could not be further confirmed by classical gating approaches.
616 Increased levels of T-cells could be related with the active role of CD8⁺T cells in the
617 esophageal inflammation in EoE^{30,31} while the change in CD4⁺CD8⁻ T-cells might be
618 associated with their cytotoxic activity as described for other pathologies³², despite no
619 role for these cells has been found in EoE.

620 PPI therapy is widely used in the management of EoE^{16,33}, with a histologic remission
621 rate of approximately 50%¹⁶. The reduction in Th2 signalling produced by this therapy
622 leads to an improvement in the structural characteristics of the esophagus,
623 accompanied by decreased eosinophil count. In our study, non-responding patients
624 presented significant differences from responding patients (Figure 3A). When we
625 studied these two groups PrePPI intake, non-responding patients had lower levels of
626 pDCs, classical monocytes and an unknown myeloid APC cluster, but higher levels of
627 non-memory B cells, mature NK cells and central memory CD4⁺ T-cells. These results
628 might indicate an increased antigen presentation activity, since they have decreased
629 numbers of circulating APC populations, which are key in homeostasis and allergy
630 response³⁴. Indeed, latest results from our group³⁵ reinforce this hypothesis showing
631 that non-responding patients' esophageal proteomic profile when compared to
632 responding patients (both PrePPI), have increased levels of proteins associated with
633 antigen presentation. These patients might have a more altered barrier in the
634 esophagus, which increases the risk of antigen exposure, thereby favouring EoE
635 worsening, as described before³⁶⁻³⁸. Although these findings need a deeper
636 characterization, they unveil for the first time a differential immunological profile
637 between patients that will or will not respond to PPI therapy and could open the door to
638 a better profiling of refractory patients.

639 In addition, when we studied immune dynamics during PPI treatment, PPI-responding
640 patients displayed a significant increase in circulating basophils (C-14) and pDCs (C-
641 26) (Figure 4A). Basophils have a pivotal role in atopic diseases and are a major
642 source of Th2 immunomodulation. The increased levels of these cells in patients who
643 achieve remission after PPI therapy could be related to the reestablishment of
644 immunological homeostasis, since during inflammation basophils are able to penetrate
645 the inflamed esophagus³⁹. A similar role may be played by circulating pDCs, which
646 recover control values in PPI-responding patients PostPPI (Figure 5A). pDCs produce
647 high levels of IFN- $\alpha\beta$ (type I). This cytokine impairs Th2 responses by blocking the

648 normal development of Th2 cells and production of Th2 cytokines (especially IL-5)^{40,41}.
649 The reduction in circulating pDCs during active esophageal inflammation could be
650 indicating migration of these cells to the inflamed tissue to control the inflammatory
651 response. Conceivably, circulating levels of these cells are restored when the patient
652 achieves remission.

653 Importantly, the chemokine receptors CXCR3 and CCR7 related to pDC migration to
654 tissues and homing to the LN^{28,29,42} were expressed in circulating pDCs (Figure 6A) in
655 our cohorts. Indeed, responders presented the most activated pDCs after PPI
656 treatment (Figure 5B) while no significant changes were found in the case of non-
657 responding patients. Together with the previous results, the observed low levels of
658 pDCs in PrePPI and PostPPI non-responding patients (Figure 5A) and their less active
659 circulating profile (Figure 6B), could be linked to a poor inhibition of the Th2 response
660 by type I IFN or/and a more exacerbated mucosal barrier alteration and therefore a
661 worse prognosis^{36,40}.

662 Focusing on promising minimally invasive biomarkers, pDCs are a potentially
663 interesting candidate since they are highly related with EoE onset and the response to
664 treatment. We have observed an inverse correlation between circulating pDCs and the
665 peak eosinophil count in esophageal biopsies (Figure 5B). Moreover, when we
666 evaluated tissue pDC levels in patient's biopsies we found a positive correlation
667 between these cells and the proportion of eosinophils per mm² (Figure 7D), being also
668 inversely correlated to pDC circulating levels (Figure 7E). In patients, the number of
669 tissue pDCs was higher when the esophageal inflammation was active, reducing their
670 abundance when the inflammation was under control (Figure 7C). However, Responder
671 patients do not reach control values after treatment despite pDC levels tend to be
672 lower. This could be due to a non-complete recovery state, in which these cells
673 participate in the restoration of the esophageal homeostasis as happens in other
674 pathologies⁴³ where tissue healing plays a key role. Thus, it may be that the evaluation
675 of tissue pDC levels in long-term recovered patients would reveal closer numbers to
676 the control.

677 Hence, this population is related with the inflammatory status of the esophagus, thus
678 providing information of clinical diagnostic parameters that until now can only be
679 measured through invasive procedures. In peripheral blood, previous works have
680 related an increase in Th2 profile to active EoE⁴⁴, while others have associated this to
681 eosinophil phenotype or maturation state^{45,46}. Also, single cell studies have described
682 T-cell heterogeneity in the inflamed tissue, defining a specific enrichment in resident
683 CD4⁺ T regulatory and Th2 effector cells together with an increased CD4⁺/CD8⁺
684 circulating T-cell ratio⁴⁷. Nevertheless, none of these parameters is being used as
685 biomarker for EoE diagnosis, or for the prediction of response to PPI treatment, for
686 which the peripheral eosinophil count has been proposed as a possible predictor⁴⁸.

687 We are aware that advances in biomarker discovery in EoE are hampered by several
688 pitfalls, such as the common concurrence of atopic diseases and the dissociation
689 between the esophageal inflammation and patient's symptoms²³. Accordingly, despite
690 our cohorts are highly controlled and paired samples from the same patients were
691 analysed, further studies and validations are needed to confirm the utility of circulating
692 pDCs as biomarker. The activity of this cluster must be compared in cohorts with other
693 allergic and atopic conditions, since in these pathologies a decreased peripheral pDC
694 count was found, together with pDC infiltration in the inflamed tissue⁴⁹⁻⁵¹. Probably, its
695 visualization through classic cytometry approaches and its combination with other non-

696 invasive clinical parameters would be helpful to establish a specific signature for EoE
697 management and PPI response prediction, also opening the door to study its utility in
698 the case of other therapy options for EoE.

699 In summary, we have described, for the first time to our knowledge, the circulating
700 immunome of EoE patients at the time of diagnosis highlighting as well the differences
701 between PPI-responding and non-responding patients. Altogether, our study provides
702 new insights on EoE immunity and sheds light on the characterization of this disorder,
703 proposing a potential biomarker for diagnosis and prediction of response to treatment,
704 which could improve decisions on better treatment options.

705

706 REFERENCES

707

- 708 1. Navarro, P., Arias, Á., Arias-González, L., Laserna-Mendieta, E.J., Ruiz-Ponce, M., and
709 Lucendo, A.J. (2019). Systematic review with meta-analysis: the growing incidence and
710 prevalence of eosinophilic oesophagitis in children and adults in population-based
711 studies. *Aliment Pharmacol Ther* *49*, 1116–1125. [10.1111/APT.15231](https://doi.org/10.1111/APT.15231).
- 712 2. Arias, Á., and Lucendo, A.J. (2019). Incidence and prevalence of eosinophilic
713 oesophagitis increase continuously in adults and children in Central Spain: A 12-year
714 population-based study. *Dig Liver Dis* *51*, 55–62. [10.1016/J.DLD.2018.07.016](https://doi.org/10.1016/J.DLD.2018.07.016).
- 715 3. Lucendo, A.J., Molina-Infante, J., Arias, Á., von Arnim, U., Bredenoord, A.J., Bussmann,
716 C., Amil Dias, J., Bove, M., González-Cervera, J., Larsson, H., et al. (2017). Guidelines on
717 eosinophilic esophagitis: evidence-based statements and recommendations for
718 diagnosis and management in children and adults. *United European Gastroenterol J* *5*,
719 335–358. [10.1177/2050640616689525](https://doi.org/10.1177/2050640616689525).
- 720 4. Hirano, I., Chan, E.S., Rank, M.A., Sharaf, R.N., Stollman, N.H., Stukus, D.R., Wang, K.,
721 Greenhawt, M., Falck-Ytter, Y.T., Chachu, K.A., et al. (2020). AGA Institute and the Joint
722 Task Force on Allergy-Immunology Practice Parameters Clinical Guidelines for the
723 Management of Eosinophilic Esophagitis. *Gastroenterology* *158*, 1776–1786.
724 [10.1053/J.GASTRO.2020.02.038](https://doi.org/10.1053/J.GASTRO.2020.02.038).
- 725 5. Schoepfer, A., and Safroneeva, E. (2014). Activity assessment of eosinophilic
726 esophagitis. *Dig Dis* *32*, 98–101. [10.1159/000357081](https://doi.org/10.1159/000357081).
- 727 6. McCormick, J.P., and Lee, J.T. (2021). Insights into the Implications of Coexisting Type 2
728 Inflammatory Diseases. *J Inflamm Res* *14*, 4259–4266. [10.2147/JIR.S311640](https://doi.org/10.2147/JIR.S311640).
- 729 7. González-Cervera, J., Arias, Á., Redondo-González, O., Cano-Mollinedo, M.M.,
730 Terreehorst, I., and Lucendo, A.J. (2017). Association between atopic manifestations
731 and eosinophilic esophagitis: A systematic review and meta-analysis. *Annals of Allergy,*
732 *Asthma and Immunology* *118*, 582-590.e2. [10.1016/j.anai.2017.02.006](https://doi.org/10.1016/j.anai.2017.02.006).
- 733 8. Greuter, T., Alexander, J.A., Straumann, A., and Katzka, D.A. (2018). Diagnostic and
734 Therapeutic Long-term Management of Eosinophilic Esophagitis—Current Concepts and
735 Perspectives for Steroid Use. *Clin Transl Gastroenterol* *9*. [10.1038/S41424-018-0074-8](https://doi.org/10.1038/S41424-018-0074-8).
- 736 9. Molina-Infante, J., and Lucendo, A.J. (2017). Proton Pump Inhibitor Therapy for
737 Eosinophilic Esophagitis: A Paradigm Shift. *Am J Gastroenterol* *112*, 1770–1773.
738 [10.1038/AJG.2017.404](https://doi.org/10.1038/AJG.2017.404).

- 739 10. Laserna-Mendieta, E.J., Casabona, S., Savarino, E., Perelló, A., Pérez-Martínez, I.,
740 Guagnozzi, D., Barrio, J., Guardiola, A., Asensio, T., de la Riva, S., et al. (2020). Efficacy of
741 Therapy for Eosinophilic Esophagitis in Real-World Practice. *Clin Gastroenterol Hepatol*
742 *18*, 2903-2911.e4. 10.1016/J.CGH.2020.01.024.
- 743 11. Molina-Infante, J., and Lucendo, A.J. (2020). Approaches to diet therapy for eosinophilic
744 esophagitis. *Curr Opin Gastroenterol* *36*, 359–363. 10.1097/MOG.0000000000000645.
- 745 12. Molina-Infante, J., Bredenoord, A.J., Cheng, E., Dellon, E.S., Furuta, G.T., Gupta, S.K.,
746 Hirano, I., Katzka, D.A., Moawad, F.J., Rothenberg, M.E., et al. (2016). Proton pump
747 inhibitor-responsive oesophageal eosinophilia: an entity challenging current diagnostic
748 criteria for eosinophilic oesophagitis. *Gut* *65*, 521–531. 10.1136/GUTJNL-2015-310991.
- 749 13. Dellon, E.S., Rothenberg, M.E., Collins, M.H., Hirano, I., Chehade, M., Bredenoord, A.J.,
750 Lucendo, A.J., Spergel, J.M., Aceves, S., Sun, X., et al. (2022). Dupilumab in Adults and
751 Adolescents with Eosinophilic Esophagitis. *N Engl J Med* *387*, 2317–2330.
752 10.1056/NEJMOA2205982.
- 753 14. Uchida, A.M., Burk, C.M., Rothenberg, M.E., Furuta, G.T., and Spergel, J.M. (2023).
754 Recent advances in the treatment of eosinophilic esophagitis. *J Allergy Clin Immunol*
755 *Pract O*. 10.1016/j.jaip.2023.06.035.
- 756 15. Laserna-Mendieta, E.J., Navarro, P., Casabona-Francés, S., Savarino, E. V., Pérez-
757 Martínez, I., Guagnozzi, D., Barrio, J., Perello, A., Guardiola-Arévalo, A., Betoré-Glaria,
758 M.E., et al. (2023). Differences between childhood- and adulthood-onset eosinophilic
759 esophagitis: An analysis from the EoE connect registry. *Dig Liver Dis* *55*, 350–359.
760 10.1016/J.DLD.2022.09.020.
- 761 16. Laserna-Mendieta, E.J., Casabona, S., Guagnozzi, D., Savarino, E., Perelló, A., Guardiola-
762 Arévalo, A., Barrio, J., Pérez-Martínez, I., Lund Krarup, A., Alcedo, J., et al. (2020).
763 Efficacy of proton pump inhibitor therapy for eosinophilic oesophagitis in 630 patients:
764 results from the EoE connect registry. *Aliment Pharmacol Ther* *52*, 798–807.
765 10.1111/APT.15957.
- 766 17. Van Rhijn, B.D., Warners, M.J., Curvers, W.L., Van Lent, A.U., Bekkali, N.L., Takkenberg,
767 R.B., Kloek, J.J., Bergman, J.J.G.H.M., Fockens, P., and Bredenoord, A.J. (2014).
768 Evaluating the endoscopic reference score for eosinophilic esophagitis: moderate to
769 substantial intra- and interobserver reliability. *Endoscopy* *46*, 1049–1055. 10.1055/S-
770 0034-1377781.
- 771 18. Lucendo, A.J., and Molina-Infante, J. (2016). Limitation of Symptoms as Predictors of
772 Remission in Eosinophilic Esophagitis: The Need to Go Beyond Endoscopy and
773 Histology. *Gastroenterology* *150*, 547–549. 10.1053/J.GASTRO.2016.01.014.
- 774 19. Wen, T., Stucke, E.M., Grotjan, T.M., Kemme, K.A., Abonia, J.P., Putnam, P.E., Franciosi,
775 J.P., Garza, J.M., Kaul, A., King, E.C., et al. (2013). Molecular diagnosis of eosinophilic
776 esophagitis by gene expression profiling. *Gastroenterology* *145*, 1289–1299.
777 10.1053/J.GASTRO.2013.08.046.
- 778 20. Rochman, M., Wen, T., Kotliar, M., Dexheimer, P.J., Morgenstern, N.B.B., Caldwell, J.M.,
779 Lim, H.W., and Rothenberg, M.E. (2022). Single-cell RNA-Seq of human esophageal

- 780 epithelium in homeostasis and allergic inflammation. *JCI Insight* 7.
781 10.1172/JCI.INSIGHT.159093.
- 782 21. Rochman, M., Azouz, N.P., and Rothenberg, M.E. (2018). Epithelial origin of eosinophilic
783 esophagitis. *Journal of Allergy and Clinical Immunology* 142, 10–23.
784 10.1016/J.JACI.2018.05.008.
- 785 22. Molina-Jiménez, F., Ugalde-Triviño, L., Arias-González, L., Relaño-Rupérez, C., Casabona,
786 S., Pérez-Fernández, M.T., Martín-Domínguez, V., Fernández-Pacheco, J.,
787 Laserna-Mendieta, E.J., Muñoz-Hernández, P., et al. (2023). Proteomic analysis of the
788 esophageal epithelium reveals key features of eosinophilic esophagitis
789 pathophysiology. *Allergy*. 10.1111/ALL.15779.
- 790 23. Rossi, C.M., Lenti, M.V., and Di Sabatino, A. (2022). The need for a reliable non-invasive
791 diagnostic biomarker for eosinophilic oesophagitis. *Lancet Gastroenterol Hepatol* 7,
792 202–203. 10.1016/S2468-1253(21)00468-4.
- 793 24. Hirano, I., Moy, N., Heckman, M.G., Thomas, C.S., Gonsalves, N., and Achem, S.R.
794 (2013). Endoscopic assessment of the oesophageal features of eosinophilic
795 oesophagitis: validation of a novel classification and grading system. *Gut* 62, 489–495.
796 10.1136/GUTJNL-2011-301817.
- 797 25. Collins, M.H., Martin, L.J., Alexander, E.S., Todd Boyd, J., Sheridan, R., He, H., Pentiuik,
798 S., Putnam, P.E., Abonia, J.P., Mukkada, V.A., et al. (2017). Newly developed and
799 validated eosinophilic esophagitis histology scoring system and evidence that it
800 outperforms peak eosinophil count for disease diagnosis and monitoring. *Dis Esophagus*
801 30. 10.1111/DOTE.12470.
- 802 26. Park, L.M., Lannigan, J., and Jaimes, M.C. (2020). OMIP-069: Forty-Color Full Spectrum
803 Flow Cytometry Panel for Deep Immunophenotyping of Major Cell Subsets in Human
804 Peripheral Blood. *Cytometry A* 97, 1044–1051. 10.1002/CYTO.A.24213.
- 805 27. McInnes, L., Healy, J., Saul, N., and Großberger, L. (2018). UMAP: Uniform Manifold
806 Approximation and Projection. *J Open Source Softw* 3, 861. 10.21105/JOSS.00861.
- 807 28. Vanbervliet, B., Bendriss-Vermare, N., Massacrier, C., Homey, B., De Bouteiller, O.,
808 Brière, F., Trinchieri, G., and Caux, C. (2003). The Inducible CXCR3 Ligands Control
809 Plasmacytoid Dendritic Cell Responsiveness to the Constitutive Chemokine Stromal
810 Cell-derived Factor 1 (SDF-1)/CXCL12. *J Exp Med* 198, 823. 10.1084/JEM.20020437.
- 811 29. Seth, S., Oberdörfer, L., Hyde, R., Hoff, K., Thies, V., Worbs, T., Schmitz, S., and Förster,
812 R. (2011). CCR7 Essentially Contributes to the Homing of Plasmacytoid Dendritic Cells to
813 Lymph Nodes under Steady-State As Well As Inflammatory Conditions. *The Journal of*
814 *Immunology* 186, 3364–3372. 10.4049/JIMMUNOL.1002598.
- 815 30. Anilkumar, A.A., Beppu, L., Kurten, R., Newbury, R., Dohil, R., Broide, D., and Aceves,
816 S.S. (2014). CD3 and CD8 Cells Produce IL-9 In Pediatric Eosinophilic Esophagitis. *Journal*
817 *of Allergy and Clinical Immunology* 133, AB288. 10.1016/j.jaci.2013.12.1017.
- 818 31. Abdolahi, M., Rasouli, S., Babaie, D., Dara, N., Imanzadeh, F., Sayyari, A., Rouhani, P.,
819 Khatami, K., Kazemiaghdam, M., Nilipour, Y., et al. (2021). Increased regulatory T cells in
820 peripheral blood of children with eosinophilic esophagitis. *Gastroenterol Hepatol Bed*
821 *Bench* 14, 25–30.

- 822 32. Wu, Z., Zheng, Y., Sheng, J., Han, Y., Yang, Y., Pan, H., and Yao, J. (2022). CD3+CD4-CD8-
823 (Double-Negative) T Cells in Inflammation, Immune Disorders and Cancer. *Front*
824 *Immunol* 13, 388. 10.3389/FIMMU.2022.816005/BIBTEX.
- 825 33. Chang, J.W., Saini, S.D., Mellinger, J.L., Chen, J.W., Zikmund-Fisher, B.J., and Rubenstein,
826 J.H. (2019). Management of eosinophilic esophagitis is often discordant with guidelines
827 and not patient-centered: results of a survey of gastroenterologists. *Dis Esophagus* 32.
828 10.1093/DOTE/DOY133.
- 829 34. Schülke, S., Gilles, S., Jirno, A.C., and Mayer, J.U. (2023). Tissue-specific
830 antigen-presenting cells contribute to distinct phenotypes of allergy. *Eur J Immunol*,
831 2249980. 10.1002/EJI.202249980.
- 832 35. Molina-Jiménez, F., Ugalde-Triviño, L., Arias-González, L., Relaño-Rupérez, C., Casabona,
833 S., Moreno-Monteagudo, J.A., Pérez-Fernández, M.T., Martín-Domínguez, V.,
834 Fernández-Pacheco, J., Laserna-Mendieta, E.J., et al. (2023). Proton pump Inhibitor
835 effect on esophageal protein signature of eosinophilic esophagitis, prediction and
836 evaluation of treatment response. *medRxiv*, 2023.11.21.23298292.
837 10.1101/2023.11.21.23298292.
- 838 36. Chen, J., Oshima, T., Huang, X., Tomita, T., Fukui, H., and Miwa, H. (2022). Esophageal
839 Mucosal Permeability as a Surrogate Measure of Cure in Eosinophilic Esophagitis. *J Clin*
840 *Med* 11. 10.3390/JCM11144246.
- 841 37. Furuta, G.T., Fillon, S.A., Williamson, K.M., Robertson, C.E., Stevens, M.J., Aceves, S.S.,
842 Arva, N.C., Chehade, M., Collins, M.H., Davis, C.M., et al. (2023). Mucosal Microbiota
843 Associated With Eosinophilic Esophagitis and Eosinophilic Gastritis. *J Pediatr*
844 *Gastroenterol Nutr* 76, 347–354. 10.1097/MPG.0000000000003685.
- 845 38. Kleuskens, M.T.A., Bek, M.K., Al Halabi, Y., Blokhuis, B.R.J., Diks, M.A.P., Haasnoot, M.L.,
846 Garssen, J., Bredenoord, A.J., C.A.M. van Esch, B., and Redegeld, F.A. (2023). Mast cells
847 disrupt the function of the esophageal epithelial barrier. *Mucosal Immunol*.
848 10.1016/J.MUCIMM.2023.06.001.
- 849 39. Marković, I., and Savvides, S.N. (2020). Modulation of Signaling Mediated by TSLP and
850 IL-7 in Inflammation, Autoimmune Diseases, and Cancer. *Front Immunol* 11.
851 10.3389/FIMMU.2020.01557.
- 852 40. Pritchard, A.L., Carroll, M.L., Burel, J.G., White, O.J., Phipps, S., and Upham, J.W. (2012).
853 Innate IFNs and Plasmacytoid Dendritic Cells Constrain Th2 Cytokine Responses to
854 Rhinovirus: A Regulatory Mechanism with Relevance to Asthma. *The Journal of*
855 *Immunology* 188, 5898–5905. 10.4049/JIMMUNOL.1103507.
- 856 41. Lin, J.Y., Wu, W.H., Chen, J.S., Liu, I.L., Chiu, H.L., Chen, H.W., Tsai, T.L., Huang, Y.L., and
857 Wang, L.F. (2020). Plasmacytoid dendritic cells suppress Th2 responses induced by
858 epicutaneous sensitization. *Immunol Cell Biol* 98, 215–228. 10.1111/IMCB.12315.
- 859 42. Kohrgruber, N., Gröger, M., Meraner, P., Kriehuber, E., Petzelbauer, P., Brandt, S.,
860 Stingl, G., Rot, A., and Maurer, D. (2004). Plasmacytoid Dendritic Cell Recruitment by
861 Immobilized CXCR3 Ligands. *The Journal of Immunology* 173, 6592–6602.
862 10.4049/JIMMUNOL.173.11.6592.

- 863 43. Gregorio, J., Meller, S., Conrad, C., Di Nardo, A., Homey, B., Lauerma, A., Arai, N., Gallo,
864 R.L., DiGiovanni, J., and Gilliet, M. (2010). Plasmacytoid dendritic cells sense skin injury
865 and promote wound healing through type I interferons. *J Exp Med* 207, 2921.
866 10.1084/JEM.20101102.
- 867 44. Adel-Patient, K., Campeotto, F., Grauso, M., Guillon, B., Moroldo, M., Venot, E.,
868 Dietrich, C., Machavoine, F., Castelli, F.A., Fenaille, F., et al. (2023). Assessment of local
869 and systemic signature of eosinophilic esophagitis (EoE) in children through multi-omics
870 approaches. *Front Immunol* 14. 10.3389/FIMMU.2023.1108895.
- 871 45. Perez-Lucendo, I., Gomez Torrijos, E., Donado, P., Melero, R., Feo-Brito, F., and Urra,
872 J.M. (2021). Low Expression of ICAM-1 in Blood Eosinophils in Patients With Active
873 Eosinophilic Esophagitis. *J Investig Allergol Clin Immunol* 31, 316–321.
874 10.18176/JIACI.0489.
- 875 46. Henderson, A., Magier, A., Schwartz, J.T., Martin, L.J., Collins, M.H., Putnam, P.E.,
876 Mukkada, V.A., Abonia, J.P., Rothenberg, M.E., and Fulkerson, P.C. (2020). Monitoring
877 Eosinophilic Esophagitis Disease Activity With Blood Eosinophil Progenitor Levels. *J*
878 *Pediatr Gastroenterol Nutr* 70, 482–488. 10.1097/MPG.0000000000002583.
- 879 47. Wen, T., Aronow, B.J., Rochman, Y., Rochman, M., Kiran, K.C., Dexheimer, P.J., Putnam,
880 P., Mukkada, V., Foote, H., Rehn, K., et al. (2019). Single-cell RNA sequencing identifies
881 inflammatory tissue T cells in eosinophilic esophagitis. *J Clin Invest* 129, 2014–2028.
882 10.1172/JCI125917.
- 883 48. Alexander, R., Alexander, J.A., Akambase, J., Harmsen, W.S., Geno, D., Tholen, C.,
884 Katzka, D.A., and Ravi, K. (2021). Proton Pump Inhibitor Therapy in Eosinophilic
885 Esophagitis: Predictors of Nonresponse. *Dig Dis Sci* 66, 3096–3104. 10.1007/S10620-
886 020-06633-4.
- 887 49. Albanesi, C., Scarponi, C., Pallotta, S., Daniele, R., Bosisio, D., Madonna, S., Fortugno, P.,
888 Gonzalvo-Feo, S., Franssen, J.D., Parmentier, M., et al. (2009). Chemerin expression
889 marks early psoriatic skin lesions and correlates with plasmacytoid dendritic cell
890 recruitment. *J Exp Med* 206, 249–258. 10.1084/JEM.20080129.
- 891 50. Saadeh, D., Kurban, M., and Abbas, O. (2016). Update on the role of plasmacytoid
892 dendritic cells in inflammatory/autoimmune skin diseases. *Exp Dermatol* 25, 415–421.
893 10.1111/EXD.12957.
- 894 51. Charles, J., Chaperot, L., Salameire, D., Domizio, J. Di, Aspor, C., Gressin, R., Jacob, M.-
895 C., Richard, M.-J., Beani, J.-C., Plumas, J., et al. (2010). Plasmacytoid dendritic cells and
896 dermatological disorders: focus on their role in autoimmunity and cancer. *Eur J*
897 *Dermatol* 20, 16. 10.1684/EJD.2010.0816.

898

899 **Supplementary Figure 1.** Hierarchical gating strategy for cluster classification.
900 Representative gating strategy used to identify the main leukocyte populations within
901 total peripheral blood mononuclear cells (PBMC). Arrows and gates are used to
902 visualize the relationships across plots. After doublets and dead cells were excluded,
903 basophils were identified as CD45+CD123+CD38+ cells. Monocytes were gated based
904 on FSC-A/SSC-A properties and further classified into non-classical (CD14–CD16+),

905 intermediate (CD14+CD16+/low), and classical (CD14+CD16-). Within the lymphocyte
906 gate, T-cells were identified based on the expression of CD3. Total $\gamma\delta$ T-cells were
907 identified as CD3+ $\gamma\delta$ T-cell receptor (TCR)+ and subdivided based on the expression
908 of CD45RA and CCR7. Total NKT-like cells were identified in the CD3+ $\gamma\delta$ TCR-
909 compartment as CD56+. The inclusion of CD2 and CD8 further classified the NKT-like
910 cells. Total T-cells were defined as CD3+ $\gamma\delta$ TCR-CD56- and further divided into CD4+,
911 CD8+, CD4+CD8+ and CD4-CD8- T-cells. Within total CD4+ T-cells and CD8+ T-
912 cells, CCR7, CD45RA, CD27, and CD28 were further used to divide them into different
913 T-cell phenotypes. B-cells were gated from the CD3- $\gamma\delta$ TCR- as CD19+ and/or CD20+
914 cells. B-cells were further classified as IgD+CD27-, IgD+CD27+, or IgD-CD27+/-; the
915 IgD-CD27+/- subset was divided into plasmablasts or IgD- memory B cells based on
916 CD20 expression and CD27. Memory cells were classified into IgM+ or IgG+. NK cells
917 were defined within the lymphocyte gate as CD3- $\gamma\delta$ TCR- and classified as early NK
918 (CD56+CD16-), mature NK (CD56+CD16+), and terminal NK (CD56-CD16+) cells.
919 Dendritic cells were identified within CD3-CD19- as CD14-CD16-. Further gating
920 identified CD123+CD45RA+ cells as plasmacytoid DCs, (pDC) and CD123-CD11c+ as
921 classical or conventional DC (cDC). cDC were divided into type 1 (CD141+, cDC1) and
922 type 2 (CD1c+, cDC2).

923

924 **Supplementary Figure 2.** Gating strategy for significant cluster validation. Statistically
925 significant cell clusters identified in Table 1 among the different comparisons performed
926 were further validated by identification following classical hierarchical gating
927 approaches. C-56 was gated from central memory CD4+ CD127+ cells. C-69 was
928 identified from early CD8 effectors as CD38+ CD314+ PD1+ CXCR3+CD95+ cells. C-
929 37 was identified from CD8-CD4- cells as CD314+ CD45RA+ CD2+ CD159a+. C-4
930 subset was identified as mature NK CD45RA+ CD314+ CD14+ CCR5+ CD2+ CD57+
931 CD159a+ cells. C-22 was gated from non-memory CD27- cell as IgM+ CXCR3- cells.
932 C-26 was defined as CD38+ CD141+ CD4+ CCR5+. C-27 was classified from classical
933 monocytes as IgG+ CD38+ CD39+ CXCR3+ CD95+ cells. C-33 was gated as CD19-
934 CD3- CD14- CD56- CXCR3+ CCR7+.

935

936 **Supplementary Figure 3.** Marker expression on the UMAP from peripheral blood
937 mononuclear cells. Surface expression intensities of all 37 analysed markers are
938 shown by a colour code based on the intensity. Red represents higher expression and
939 blue represents lower expression

940

941 **Supplementary Figure 4.** Non-Responders do not recover pDC values after
942 treatment. (A) Volcano plot of differential analysis between NR-PrePPI (n=9) and NR-
943 PostPPI (n=9). LogFC and -Log(p-value) are represented. (B) UMAP representation
944 from NR-PrePPI and PostPPI patients with pDC coloured. (C) Validation by classic
945 gating of pDC as shown in Supplementary Figures 1 and 2. Boxplot with pDC
946 represents individual percentage of total value, group median and minimum and
947 maximum values. Red line indicates paired PrePPI and PostPPI samples. Differences
948 were analysed by paired t-test analysis considering p-values <0.05 as statistically

949 significant (* $p < 0.05$) (n=7). Non-Responder (NR), before treatment (PrePPI), after
950 treatment (PostPPI).

951

952 **Supplementary Table 1.** Specificity, fluorochrome, clone and provider of the different
953 antibodies used.

954

955 **Supplementary Table 2.** Cell cluster identification from control and EoE patients. For
956 each of the 73 identified FlowSOM clusters its ontogeny and subset is shown, together
957 with the specific subset, phenotype and expression of functional markers. Markers
958 highlighted in bold denote differential expression within the same population.

959

960

961

962

963

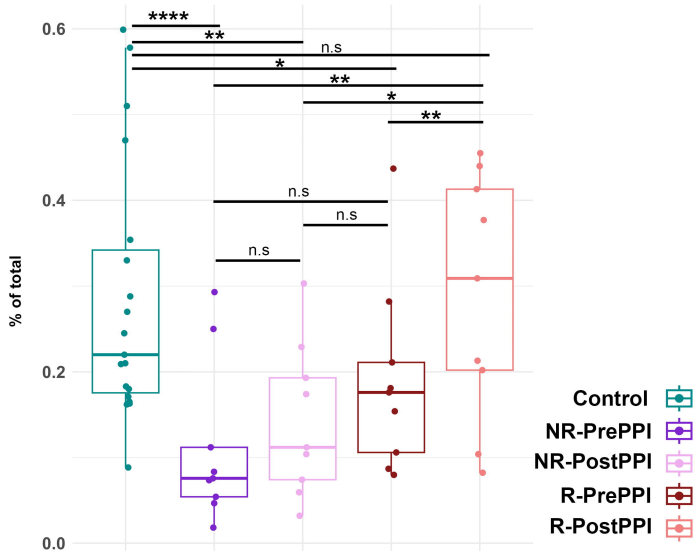
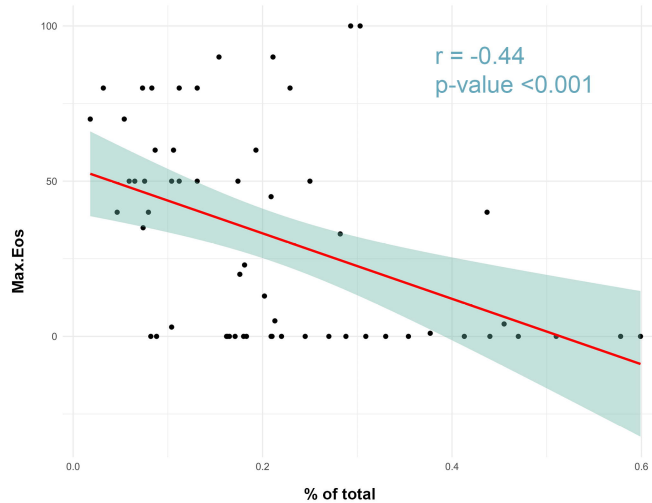
964

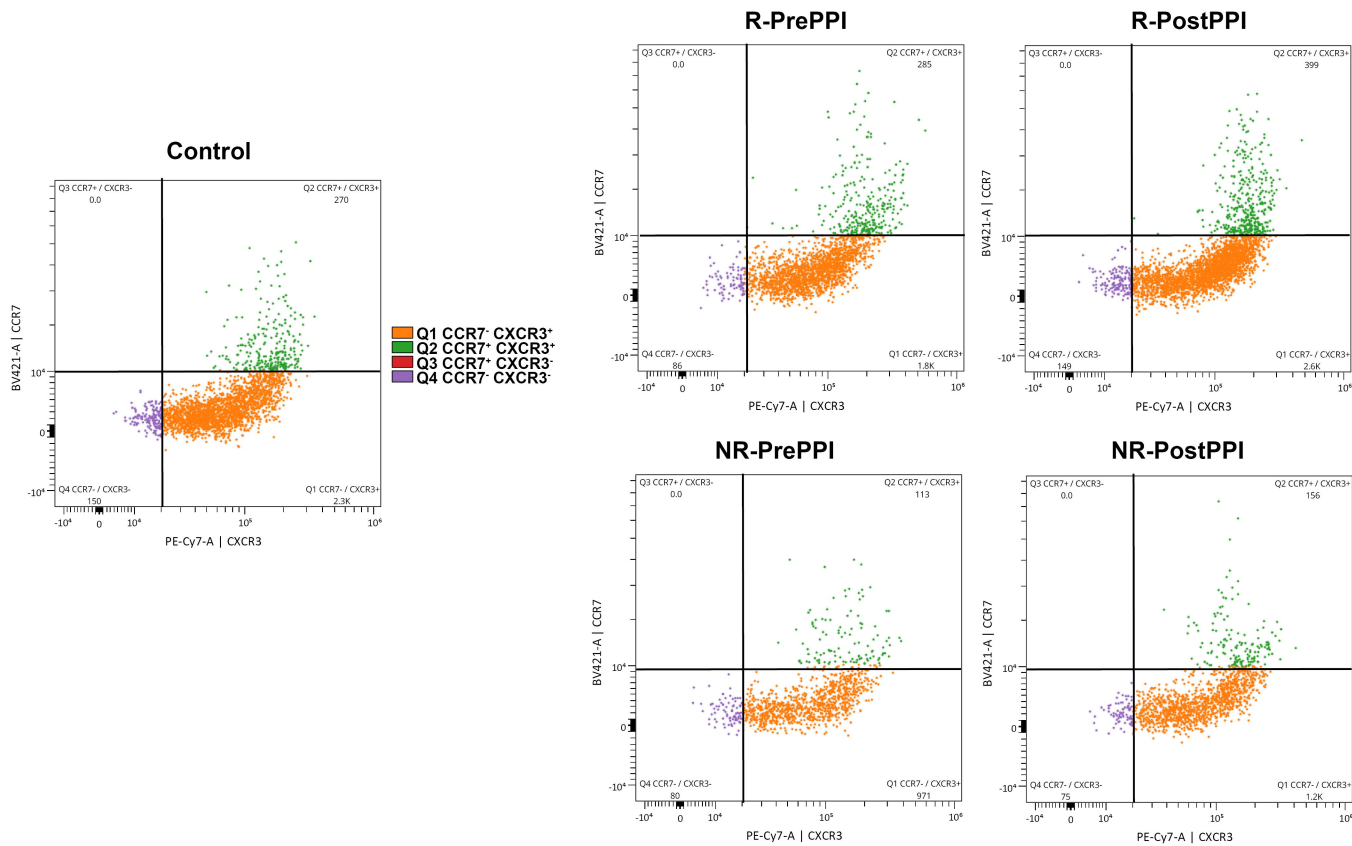
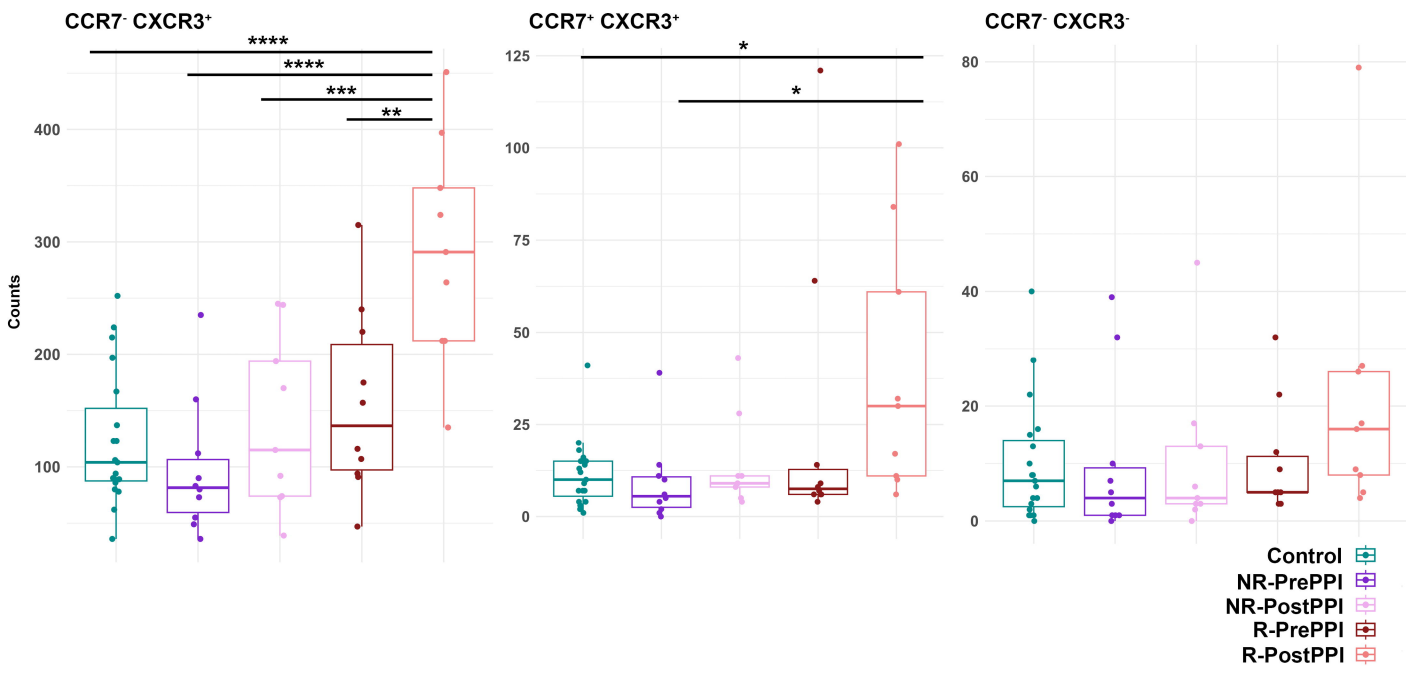
965

966

A

C-26 Dendritic cells pDC

**B**

A**B**

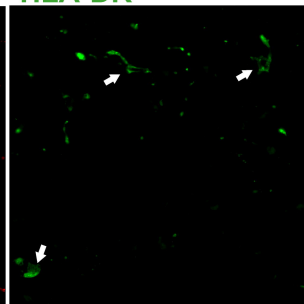
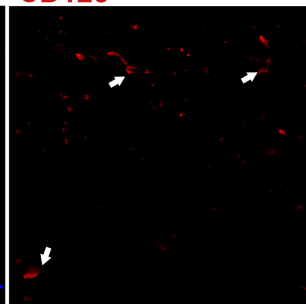
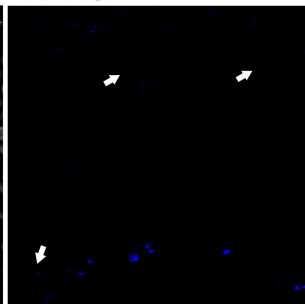
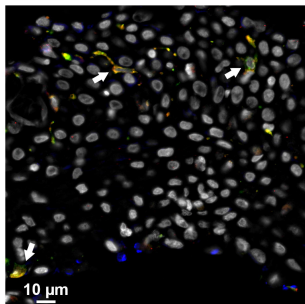
A

MERGE

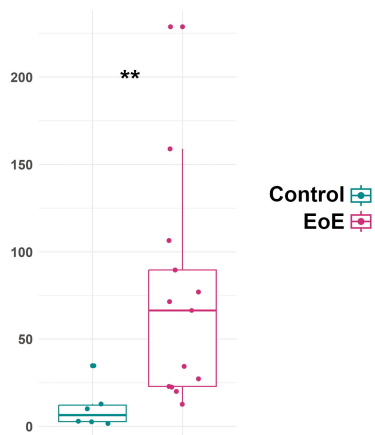
CD11c

CD123

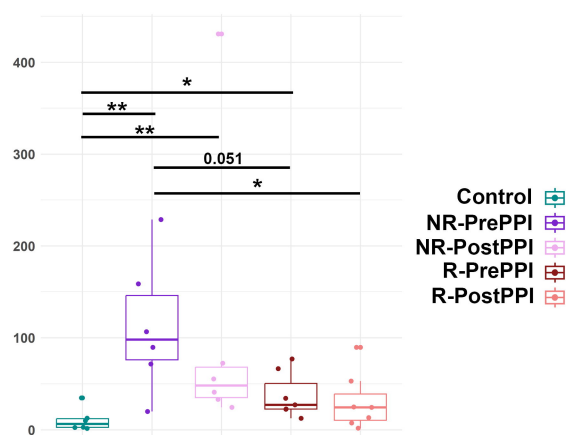
HLA-DR



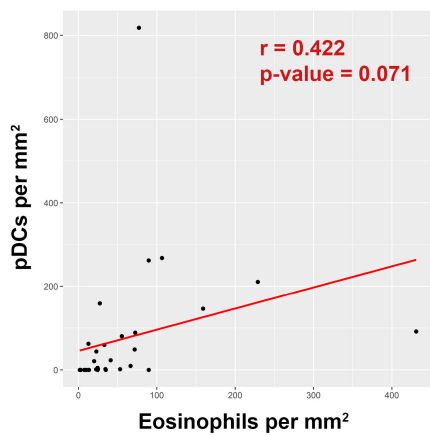
B



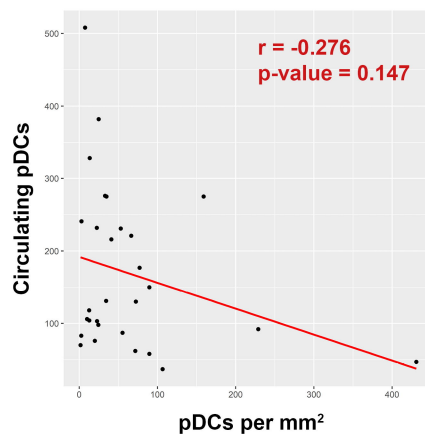
C



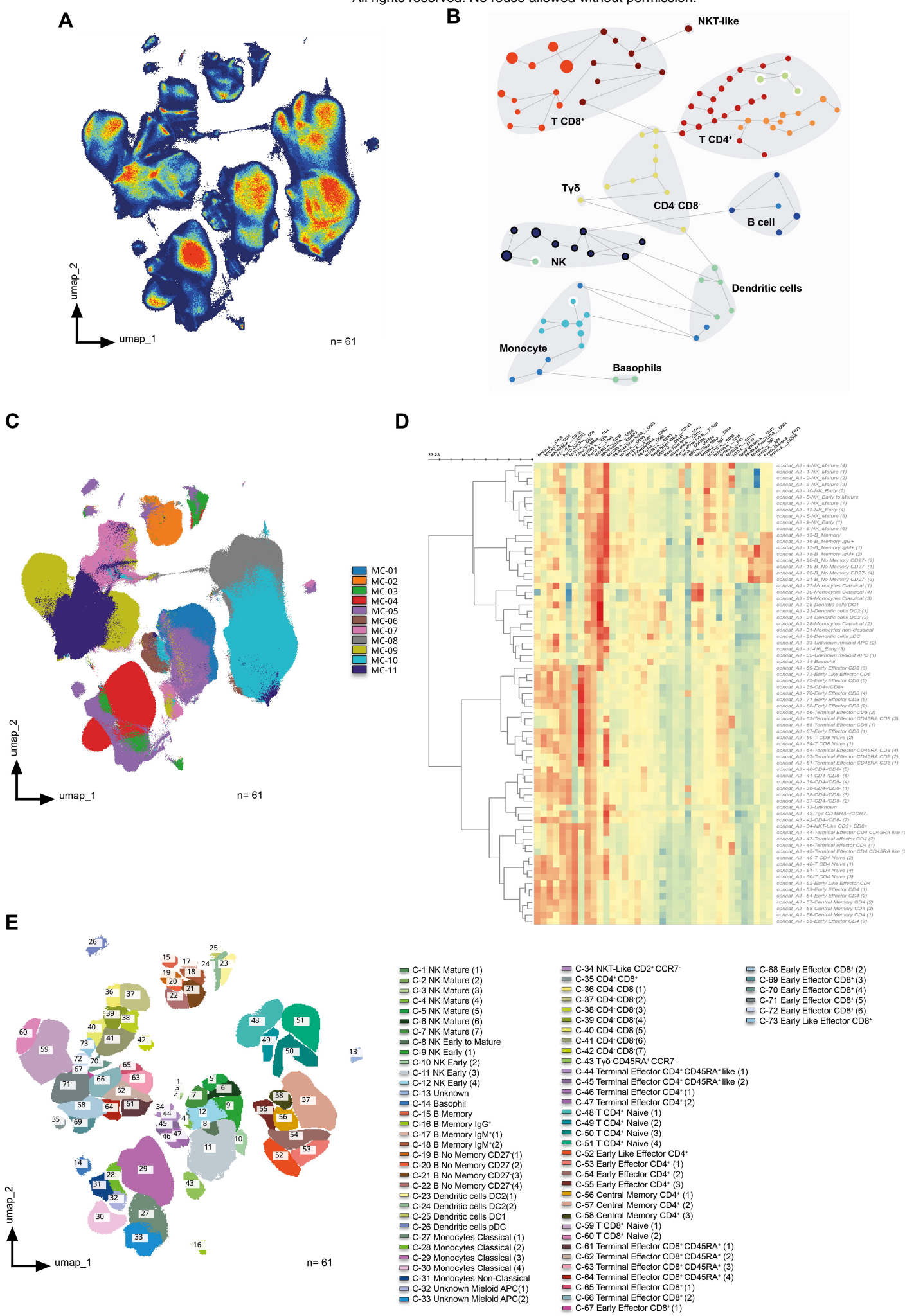
D

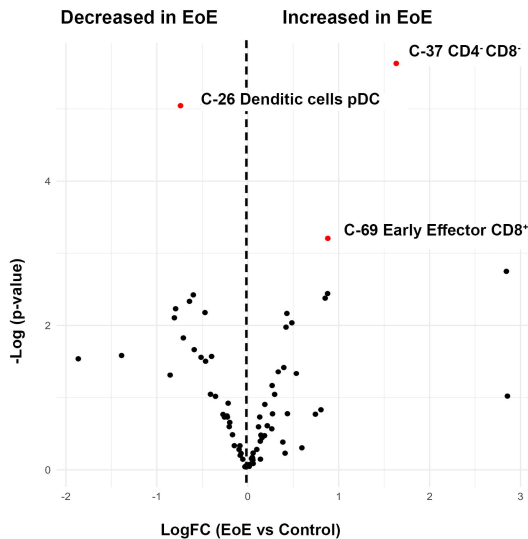
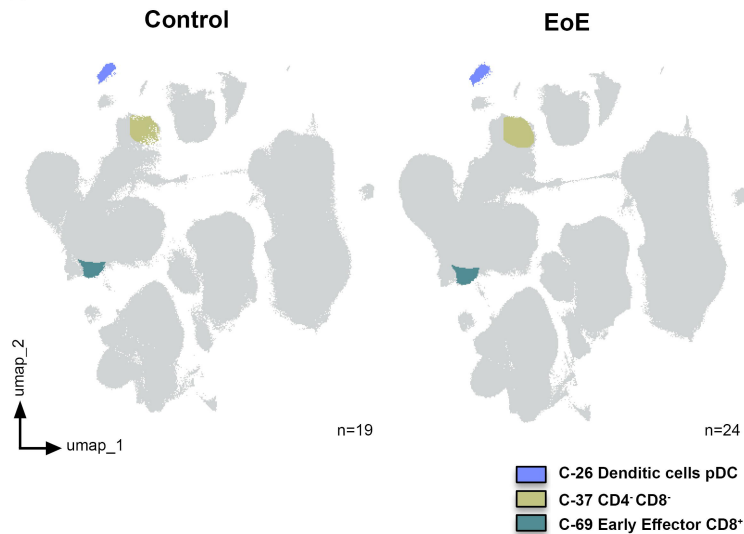
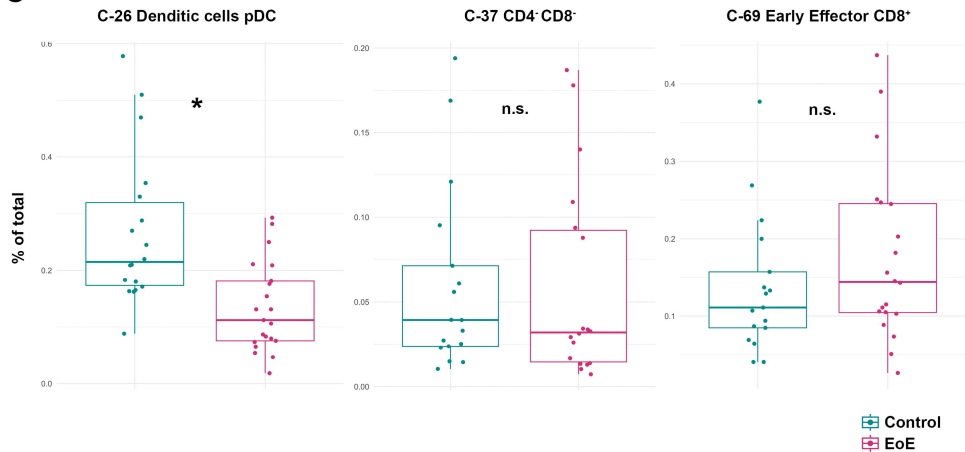


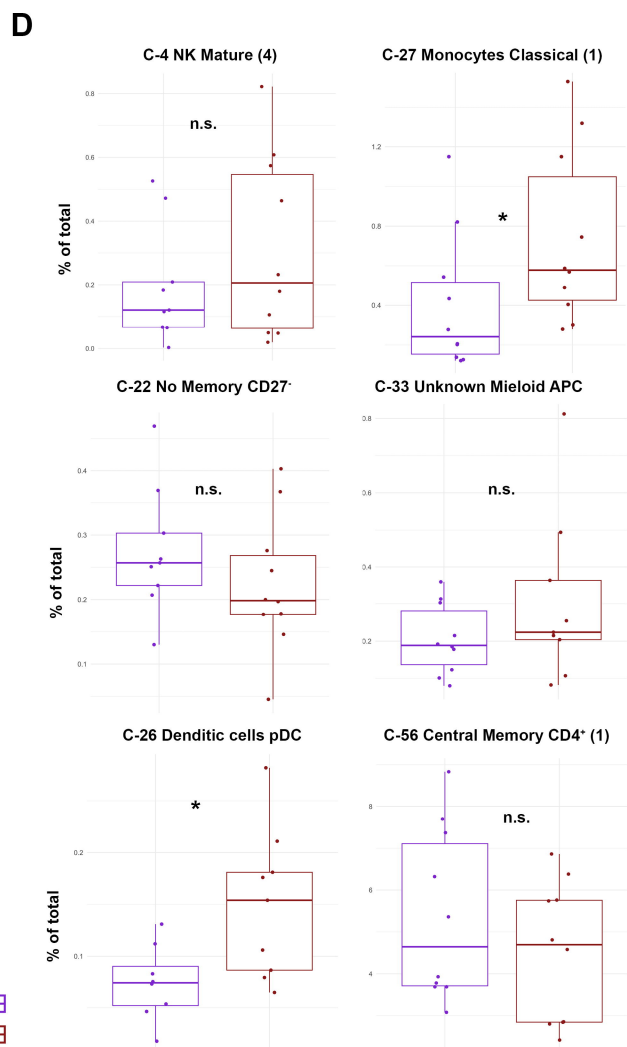
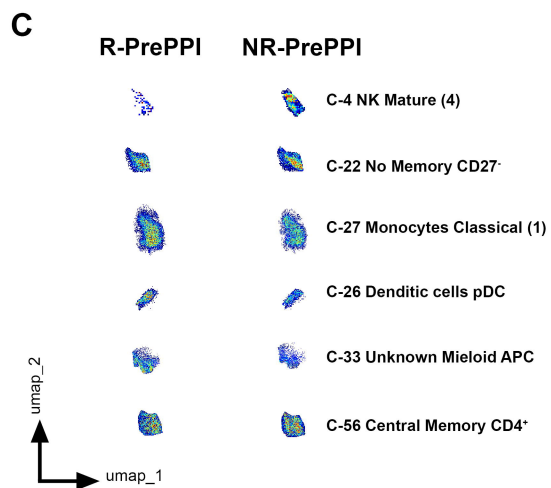
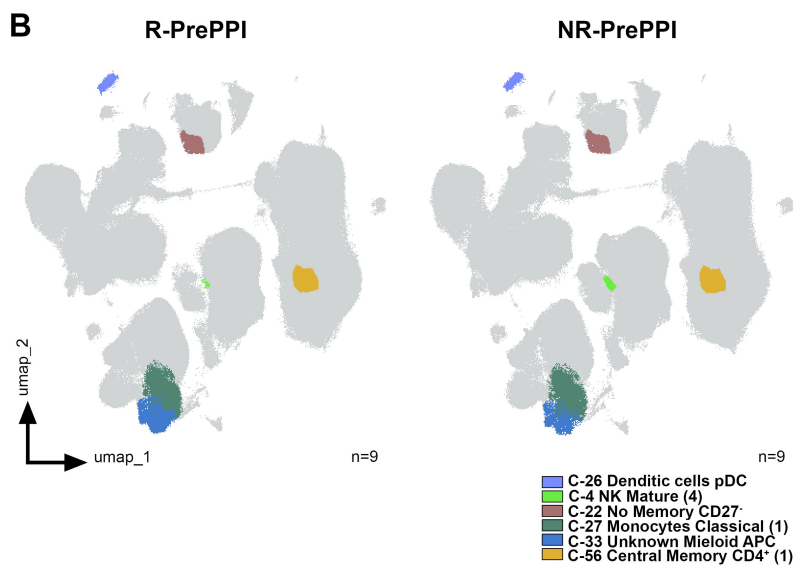
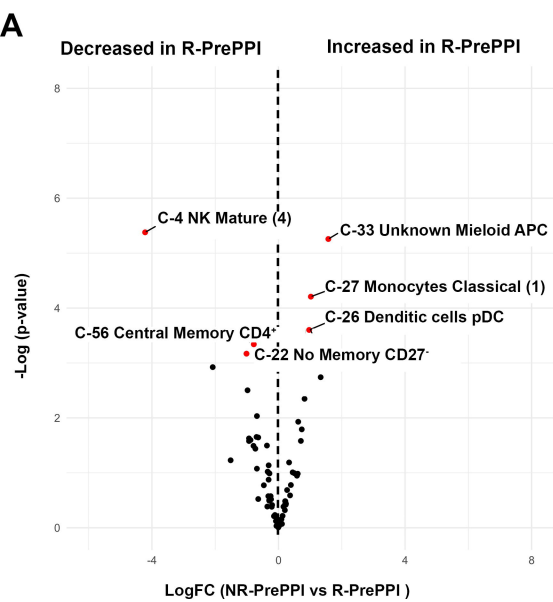
E

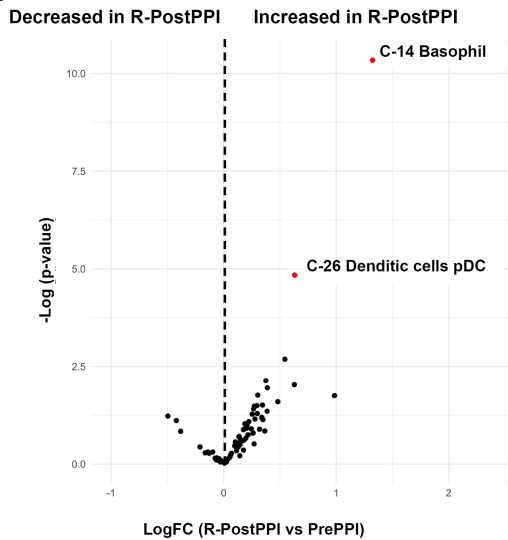
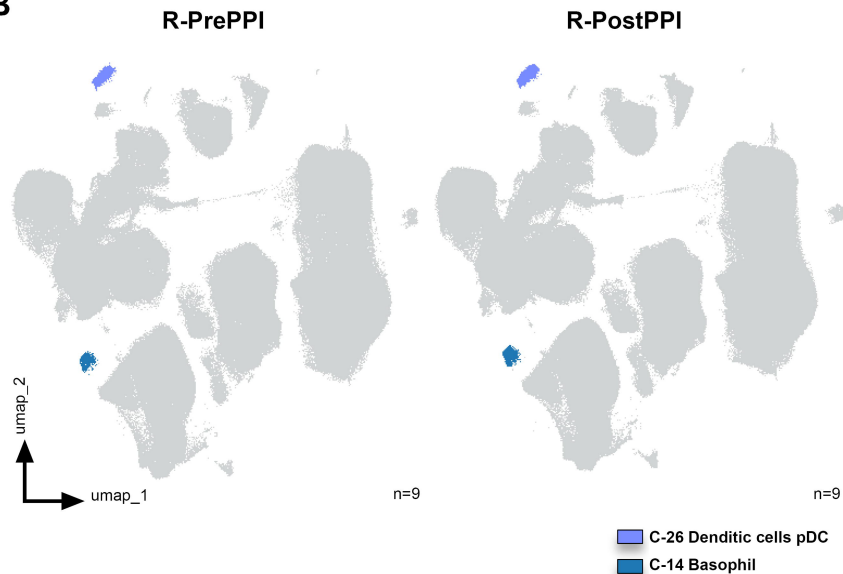


	Control (n=19)	EoE (n=25)	p-value	Responders (n=9)	Non-Responders (n=9)	p-value
Sex (male) (n,%)	13 (68%)	20 (80%)	0.488	7 (77%)	7 (77%)	1
Age (mean years \pm s.d.)	34.42 \pm 10.93	41 \pm 13.7	0.060	33 \pm 12.85	44 \pm 14.95	0.152
<i>Symptoms (n,%)</i>						
Dysphagia	0	23 (92%)	<0.001	9 (100%)	9 (100%)	1
Food impaction	0	16 (64%)	<0.001	7 (77%)	5 (55%)	0.619
Heartburn	0	10 (40%)	0.002	3 (33%)	3 (33%)	1
Abdominal pain	0	0 (0%)	1	0 (0%)	0 (0%)	1
<i>Any atopic disease (n,%)</i>						
Asthma	0	5 (22%)	0.053	3 (33%)	1 (11%)	0.573
Allergic rhinitis/sinusitis	1 (5%)	19 (82%)	<0.001	8 (88%)	9 (100%)	1
Food allergy	2 (10%)	11 (48%)	0.0173	5 (55%)	3 (33%)	0.637
<i>Endoscopic findings (n,%)</i>						
EREFS (mean \pm s.d.)	0	3.36 \pm 2	<0.001	2.44 \pm 2.06	3.88 \pm 1.26	0.097
EREFS PostPPI (mean \pm s.d.)	-	-	-	1.44 \pm 1.51	4.33 \pm 1	<0.001
Maximum eosinophil count (mean \pm s.d.)	0	55.68 \pm 23.9	<0.001	46.22 \pm 21.76	65.56 \pm 19.43	0.064
Maximum eosinophil count PostPPI (mean \pm s.d.)	-	-	-	1.44 \pm 2	65 \pm 20.91	<0.001
<i>Histological findings</i>						
EoEHSS Grade (0-1) (mean \pm s.d.)	0	0.50 \pm 0.19	<0.001	0.43 \pm 0.22	0.57 \pm 0.15	0.122
EoEHSS Grade (0-1) PostPPI (mean \pm s.d.)	-	-	-	0.06 \pm 0.04	0.40 \pm 0.22	0.006
EoEHSS Stage (0-1) (mean \pm s.d.)	0	0.47 \pm 0.16	<0.001	0.43 \pm 0.17	0.57 \pm 0.15	0.122
EoEHSS Stage (0-1) PostPPI (mean \pm s.d.)	-	-	-	0.02 \pm 0.03	0.31 \pm 0.19	0.007
<i>PPI Treatment</i>						
Omeoprazol	-	-	-	6 (66%)	2 (22%)	0.1385
Esomeprazol	-	-	-	2 (22%)	2 (22%)	
Pantoprazol	-	-	-	1 (11%)	5 (55%)	



A**B****C**



A**B****C**